MODELLING STUDY OF HIGH-CURRENT DENSITY CHLOROPHYLL-BASED DYE-SENSITIZED SOLAR CELL

ABDUL AKRAM AZFAR BIN ABD. FADZIR

BACHELOR OF ELECTRICAL ENGINEERING WITH HONOURS

UNIVERSITI MALAYSIA PAHANG

UNIVERSITI MALAYSIA PAHANG

DECLARATION OF THESIS AND COPYRIGHT

Author's Full Name : ABDUL AKRAM AZFAR BIN ABD. FADZIR

Date of Birth : 3^{RD} FEBRUARY 1998

Title : MODELLING STUDY OF HIGH-CURRENT DENSITY CHOLOROPHYLL-BASED DYE-SENSITIZED SOLAR CELL

Academic Session : SEMESTER I 2021/2022

I declare that this thesis is classified as:

☐	CONFIDENTIAL	(Contains confidential information under the Official Secret Act 1997)*
☐	RESTRICTED	(Contains restricted information as specified by the organization where research was done)*
☑	OPEN ACCESS	I agree that my thesis to be published as online open access (Full Text)

I acknowledge that Universiti Malaysia Pahang reserves the following rights:

1. The Thesis is the Property of Universiti Malaysia Pahang
2. The Library of Universiti Malaysia Pahang has the right to make copies of the thesis for the purpose of research only.
3. The Library has the right to make copies of the thesis for academic exchange.

Certified by:

(Student's Signature)	(Supervisor's Signature)
980203-11-5729	Dr Ahmad Syahiman Bin Ahmad Shah
New IC/Passport Number	Name of Supervisor
Date: 20th February 2022	Date: 21 February 2022

NOTE: * If the thesis is CONFIDENTIAL or RESTRICTED, please attach a thesis declaration letter.

THESIS DECLARATION LETTER (OPTIONAL)

Librarian,
Perpustakaan Universiti Malaysia Pahang,
Universiti Malaysia Pahang,
Lebuhraya Tun Razak,
26300, Gambang, Kuantan.

Dear Sir,

CLASSIFICATION OF THESIS AS RESTRICTED

Please be informed that the following thesis is classified as RESTRICTED for a period of three (3) years from the date of this letter. The reasons for this classification are as listed below.

Author's Name
Thesis Title

Reasons (i)

(ii)

(iii)

Thank you.

Yours faithfully,

____
(Supervisor's Signature)

Date:

Stamp:

Note: This letter should be written by the supervisor, addressed to the Librarian, *Perpustakaan Universiti Malaysia Pahang* with its copy attached to the thesis.

Universiti Malaysia PAHANG
Engineering • Technology • Creativity

SUPERVISOR'S DECLARATION

I hereby declare that I have checked this thesis and in my opinion, this thesis is adequate in terms of scope and quality for the award of the degree of Electrical Engineering (Power System).

____

(Supervisor's Signature)

Full Name : Dr Ahmad Syahiman Bin Ahmad Shah

Position : Senior Lecturer

Date : 21 February 2022

____

(Co-supervisor's Signature)

Full Name :

Position :

Date :

Universiti Malaysia PAHANG
Engineering • Technology • Creativity

STUDENT'S DECLARATION

I hereby declare that the work in this thesis is based on my original work except for quotations and citations which have been duly acknowledged. I also declare that it has not been previously or concurrently submitted for any other degree at Universiti Malaysia Pahang or any other institutions.

____

(Student's Signature)

Full Name : ABDUL AKRAM AZFAR BIN ABD. FADZIR

ID Number : EC 18098

Date : 20TH FEBRUARY 2022

MODELLING STUDY OF HIGH-CURRENT DENSITY CHLOROPHYLL-BASED DYE-SENSITIZED SOLAR CELL

ABDUL AKRAM AZFAR BIN ABD. FADZIR

Thesis submitted in fulfillment of the requirements
for the award of the
Bachelor of Electrical Engineering with Honours.

College of Engineering
UNIVERSITI MALAYSIA PAHANG

FEBRUARY 2022

ACKNOWLEDGEMENTS

All praise be to Allah SWT the only one who the most merciful for providing the strength to complete this thesis. One of the joys of a compilation is to look over the journey past and remember all the ups and downs. Thanks to all those who have given a hand on fulfilling this road.

Deserving of special mention are Dr Ahmad Syahiman Bin Mohd Shah who would have had the headache instead of myself for providing great guidance and outstanding supports in giving out ideas, teachings, and responding to each question upon completing this project.

Special thanks go for my beloved parents, Mr Abd. Fadzir and Mrs Noriza, their constant support should have received a great award and thank you to my family and my friends for the support and encouragement, and without them it was impossible for me to bring out the potential in me to give it all on this project.

Hoping that all the effort done in and out on putting this project into words would be of a great use for fellow engineers and students out there and would bring about a great inspiration.

ABSTRAK

Disebabkan kos pengeluarannya yang rendah, Sel Suria Pemeka Pewarna (*DSSC*) telah mencetuskan banyak perhatian. Banyak kajian telah dijalankan untuk menambah baik ciri dan strukturnya untuk kecekapan optimum dan faktor isian. Dalam kertas kerja ini, 10 sampel pewarna klorofil, daun Semambu, daun Aprikot, daun Betik, daun Pawpaw, daun Selasi Besar, Bayam, daun Jenjuang, daun Seri Pagi, daun Jarak Pagar dan daun *Chinar* digunakan untuk mencari ketumpatan arus-voltan (*J-V*) yang tertinggi dengan menggunakan perisian Model Peranti Fotovoltaik Tujuan Am (*GPVDM*). Jenis pewarna klorofil yang berbeza mempunyai parameter tersendiri di mana ia menghasilkan keluaran *J-V* yang berbeza. Bagi mencari parameter utama yang boleh menghasilkan *J-V* tertinggi, *GPVDM* digunakan dengan mensimulasikan semua sampel pewarna klorofil. Dalam *GPVDM*, terdapat dua data kritikal yang diperlukan sebelum memasukkan bahan pewarna; data penyerapan dan data indeks biasan bahan. Simulasi elektrik telah dibuat dengan menggunakan *GPVDM* yang menggunakan saiz kawasan aktif *DSSC* yang berbeza dengan merujuk kepada kertas penyelidikan sebelum ini. Pewarna Bayam menghasilkan simulasi *J-V* tertinggi berbanding sampel lain dengan 1.6 mA/cm^2.

ABSTRACT

Due to its low cost of production, the dye-sensitized solar cell (DSSC) has sparked a lot of attention. Many studies have been conducted to improve its features and structure for optimal efficiency and fill factor. In this paper, 10 samples of chlorophyll dye, Neem leaves, Apricot leaves, Papaya leaves, Pawpaw leaves, Scent leaves, Spinach, Ti plant leaves, Morning Glory leaves, Jatropha Curcas leaves and Chinar leaves are used in order to find the highest current density-voltage (J-V) by using General-purpose Photovoltaic General-purpose Photovoltaic Device Model (GPVDM) software. Different types of chlorophyll dye have their own parameters where they produce different output of J-V. In order to finding the main parameter that can produce the highest J-V, GPVDM is used by simulate all samples chlorophyll dye. In GPVDM, there are two main critical data are needed before inserting the dye material; absorbance data and refractive index data of the material. The electrical simulation has been made by using GPVDM which are using the different size of active area DSSC by referring to the previous research paper. Spinach dye is producing the highest simulated J-V compared to the other samples with 1.6 mA/cm^2.

TABLE OF CONTENT

LIST OF TABLES

LIST OF FIGURES

LIST OF SYMBOLS

η	Solar cell's conversion efficiency
$G(x)$	Exciton production rate
$n(\lambda)$	Refractive index
$k(\lambda)$	Extinction coefficient
c	Speed of light
Q	Absorption coefficient
E	Energy flow dissipation
h	Plank's constant
ϵ_0	Free space permittivity
ϵr	Relative permittivity
ϕ	Voltage profile
x	Dimension perpendicular to the cell surface
J_n	Electron current densities
J_p	Hole current densities
n	Electron densities
p	Hole densities
R_n	Electron recombination rate
R_p	Hole recombination rate
G	Generation rate
$D_{n/p}$	Diffusion coefficient

LIST OF ABBREVIATIONS

DSSC	Dye-Sensitized Solar Cell
J-V	Current density-voltage
GPVDM	General-purpose Photovoltaic Device Model
CdTe	Cadmium Telluride
CIGS	Copper Indium Gallium Diselenide
TCO	Transparent Conducting Oxide
Pt	Platinum
FF	Fill Factor
I_{sc}	Short-circuit Current
V_{oc}	Open-circuit Voltage
P_{in}	Incident Power
CE	Counter Electrode
PE film	Photoelectrode film
TiO_2	Titanium Dioxide
c-Si	Crystalline Silicon
GaAs	Gallium Arsenide
a-Si:H	Hydrogenated Amorphous Silicon
OLED	Organic Light-Emitting Diode
LED	Light-Emitting Diode
OFET	Organic Field-Effect Transistor
1D	One-dimensional
2D	Two-dimensional
3D	Three-dimensional
MIS	Metal-Insulator-Semiconductor
FTO	Fluorine-doped Tin Oxide
ITO	Indium Tin Oxide

CHAPTER 1

INTRODUCTION

1.1 Project Background

Dye-Sensitized Solar Cell (DSSC) is the third-generation solar cell that manipulates the concept of plant's photosynthesis in order to harvest the energy from the sunlight in whatever condition though during the low irradiance or light intensity. Chlorophyll, which can be extracted from majority of green plants, is one of the important substances in absorbing the light for energy harvesting. Chlorophyll, being the most abundant pigment that commonly found in plants, bacteria, and algae, plays a vital role in photosynthesis. Chlorophylls are natural pigments and therefore safe, environmentally friendly, easily available and cheap. A DSSC basically comprises a semiconductor that has been soaked in sensitizing dye which for this project is chlorophyll, a counter electrode, and an electrolyte containing a redox mediator. The dye absorbs light, which is transformed into electricity.

1.2 Problem Statement

In real fabrication of DSSC, it is very difficult to have an identical output current-voltage characteristics though the same badge of plants or fruits as dyes are used. Different types of chlorophyll dye have their own parameter where it produces different output of current density-voltage (J-V). Therefore, it is necessary to use simulation platform to drive the current density to it high value, ideally.

1.3 Objective

The aim of this project is:

1) To analyse the effect of variation parameter in chlorophyll layer toward DSSC performance.

2) To characterize a high current density-voltage (J-V) of chlorophyll-based DSSC.

3) To identify the photovoltaic software that can run the simulation of chlorophyll based DSSC.

1.4 Scope of Study

Scope of study are:

1) Modelling and simulation of DSSC with varying the parameter of chlorophyll layer.

2) To do the simulation and observe the DSSC performance by referring J-V curve.

1.5 Relevancy

This paper wants to verify the General-purpose Photovoltaic Device Model (GPVDM) software ability in simulating the high-current density of chlorophyll-dye based of DSSC. If this software can accurately analyse the high-current density of chlorophyll-dye based of DSSC as close as the previous experimental research value, thus this software proven reliable.

1.6 Feasibility

The feasibility of this project is to complete the project within the allocated time frame, while maintaining the consistency of this project.

During this semester (FYP 2), the scope and task that will be covered are:

1) Running the simulation for all samples of chlorophyll dye.

2) Analyse the parameter of chlorophyll dye in producing higher J-V.

CHAPTER 2

LITERATURE REVIEW

2.1 Solar Cell Generation

2.1.1 First Generation

The first generation solar cell is a silicon-based solar cell [1], due to its high efficiency, continues to dominate the solar panel market. Due to its high endurance level compared to other types of solar cells, this type of solar cell accounts for 86% of the solar market. However, producing silicon-based solar cells is quite expensive, and they lose some of their effectiveness when exposed to high temperatures, such as on a hot sunny day.

Monocrystalline solar cells, polycrystalline solar cells, amorphous silicon solar cells, and hybrid silicon solar cells are the four forms of silicon now employed in solar panel manufacturing.

2.1.2 Second Generation

In comparison to the first generation, second generation solar cells are thin film based and have a lower production cost. It does, however, have poorer efficiency. Amorphous silicon, cadmium telluride (CdTe), and copper indium gallium diselenide (CIGS) are the three kinds of this generation [1]. Non-silicon materials include CdTe and CIGS. Second-generation solar cells require less support for installing panels on rooftops, allowing for reduced cost per watt, reduced bulk, and the ability to roll the panel out onto a roof or other surface.

2.1.3 Third Generation

Third-generation solar cells vary from earlier generations in that they may be composed of a variety of materials other than silicon. The p-n junction was not used to segregate photogenerated charge carriers in this generation. Polymer solar cells, nanocrystalline solar cells, and dye-sensitized solar cells are among the prospective solar breakthroughs covered [1]. In this paper, I study the performance of DSSC by analysing J-V curve in various type of chlorophyll-based dye.

2.2 Dye-Sensitized Solar Cell (DSSC)

Nowadays, silicon-based solar cells are commonly employed, with an efficiency of around 25%. However, one of the disadvantages is the high manufacturing cost, which is more than that of fossil fuels and also difficult to construct. Michael Grätzel and Brian O'Regan of the École Polytechnique Fédérale de Lausanne invented DSSC in 1991 [2]. DSSC is an electrochemical device that uses light-absorbing dye molecules adsorbed on semiconductor particles to produce power from sunshine. DSSC consists of mesoporous nanocrystalline semiconductors such as TiO2, ZnO, and SnO2 photoanodes anchored with dye molecules that serve as light harvesters fabricated on Transparent Conducting Oxide (TCO), a platinum (Pt) counter electrode, and an electrolyte solution with dissolved iodide ion/tri-iodide ion redox couples between electrodes [3]. Dye sensitizers operate as light absorbers, then use the energy from the light to trigger a vectorial electron transfer process.

This equation may be used to express the solar cell's conversion efficiency (η) [3]:

$$\eta = FF \times I_{sc} \times {}^{V_{oc}}/_{P_{in}} \qquad 1.0$$

Where FF stands for fill factor, I_{sc} stands for short circuit current, V_{oc} is for open circuit voltage, and P_{in} is for incident power. This equation illustrates that these four factors must be modified in order to increase conversion efficiency. The sheet resistance of TCO, the resistance of ionic diffusion in the electrolyte, and the resistance at the interface between the counter electrode (CE) and the electrolyte make up the series resistance in DSSCs.

Because of their low production costs, DSSCs have the potential to be more cost effective than traditional solar cells. Cheap printing materials and easy manufacturing procedures are responsible for the low production costs. However, in addition to its shorter operational lifetime, the key concern that has been researched over the past ten years is the lower efficiency of power conversion. For the time being, some sources claim that DSSC efficiency has risen to 14%, while others claim it can achieve until 20% [4]. However, due to a lack of knowledge of the DSSC mechanism's behaviour, we were only able to obtain efficiency levels of above 14% on a few occasions. The current focus is on identifying all aspects that can result in increased energy conversion, cheaper costs, and a longer working lifetime.

2.2.1 Basic Structure

Transparent conductive oxide (TCO) layer, photoelectrode film (PE film) layer, electrolyte, and counter electrode (CE) layer makes up a typical DSSC. TCO is covered with a transparent and electrically conductive glass or plastic. A photoelectrode is a nanophorous sheet made up of linked titanium dioxide (TiO_2) particles that are dyed. These dye molecules absorb light from the sun, and TiO_2 plays a crucial role in ensuring that dye molecules are in direct contact with both TiO_2 and the electrolyte by acting as an electron acceptor and an electrical conductor [5]. The counter electrode layer is similar to the TCO layer, but it is covered with platinum catalyst particles. The structure of DSSC is depicted in Figure 1.

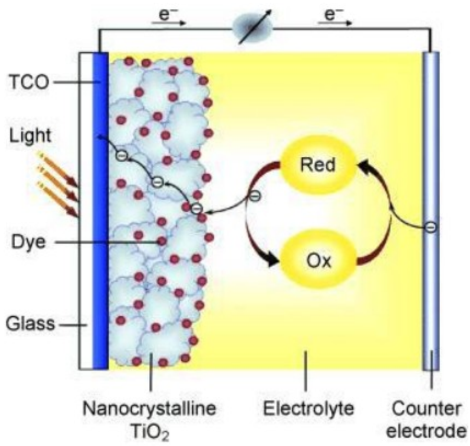

Figure 1 Basic Structure of DSSC
Source: Internet

2.3 Solar Cell Simulators

In this part, a comparative analysis of the previously stated solar cell simulators was carried out, taking into consideration the development techniques, employed programming languages, semiconductor models, and essential features from the beginning to the most recent edition.

2.3.1 SCAPS

SCAPS is also a popular 1D simulation tool for CIGS solar cells. Marc Burgelman et al. created this tool at the University of Gent in 1996 [6]. This simulator was created by combining the Gummel technique with the Newton Raphson approach for CIGS and CdTe solar cells. This programme has been shown to be particularly successful for Crystalline Silicon (c-Si), Gallium Arsenide (GaAs), Hydrogenated Amorphous Silicon (a-Si:H) cell, and micromorphous Si solar cells to date [6].

2.3.2 SETFOS

SETFOS simulator is a commercially available package for organic thin-film solar cell and Organic Light-Emitting Diode (OLED) applications. It is a very strong simulation tool created by Fluxim AG's Professor Dr. Beat Ruhstaller [7]. SETFOS incorporates four separate modules to model light emission, absorption, scattering, and charge transport properties [7]. This simulator has been identified as a viable tool for optimising the structure of organic solar cell devices. As a result, the software's dependability, speed, and flexibility make it suitable for perovskite, quantum dot, and similar organic solar cells.

2.3.3 General-purpose Photovoltaic Device Model (GPVDM)

General-purpose Photovoltaic Device Model (GPVDM) is another organic thin-film solar cell modelling programme created in 2011 by Roderick C. I. MacKenzie at Imperial College London [8]. Furthermore, this programme can mimic the performance of organic Light-Emitting Diode (LED), Organic Field-Effect Transistor (OFET), optical filters, and so on. It is a cross-platform programme that includes both electrical and optical models for producing accurate solar cell simulations [8]. This simulator's cross-platform nature makes it an ideal tool for investigating the influence of optoelectronic characteristics.

2.3.4 ATLAS

The majority of the simulators described above are designed to simulate 1D solar cells. ATLAS, on the other hand, is an excellent simulator designed for analysing the optoelectronic behaviour of 2D and 3D semiconductor devices. Silvaco Atlas created this simulator, which is used to simulate several types of single junction solar cells [9]. It also has the capability of imitating the performance of tandem cells. The optoelectronic characteristics of organic cells may also be simulated using this technology. However, this simulator can simulate the performance of textured cells, CIGS cells, 3D coaxial cells, Metal-Insulator-Semiconductor (MIS) cells, and even light detectors and image sensors [9].

2.4 Selected Solar Cell Simulator

The solar cell simulators described above are well-established and regularly used for doing simulation work on many types of solar cells. After researching all of these type simulators, General-purpose Photovoltaic Device Model (GPVDM) simulator is selected as a simulation software for this study. In order to simulate the DSSC type solar cell, the software that can simulate the 2D/3D type simulation is needed, so that the structure of the DSSC can be manipulated during the simulation. There are three type of solar cell simulator that can simulate the 2D/3D type simulation which is SETFOS, GPVDM and ATLAS. Another reason that GPVDM is used for this study, because it is an open-source software while the other two are not. Figure 2.2 shows the interface of the GPVDM and Figure 2.3 shows the type of solar cell that can be simulate using this software.

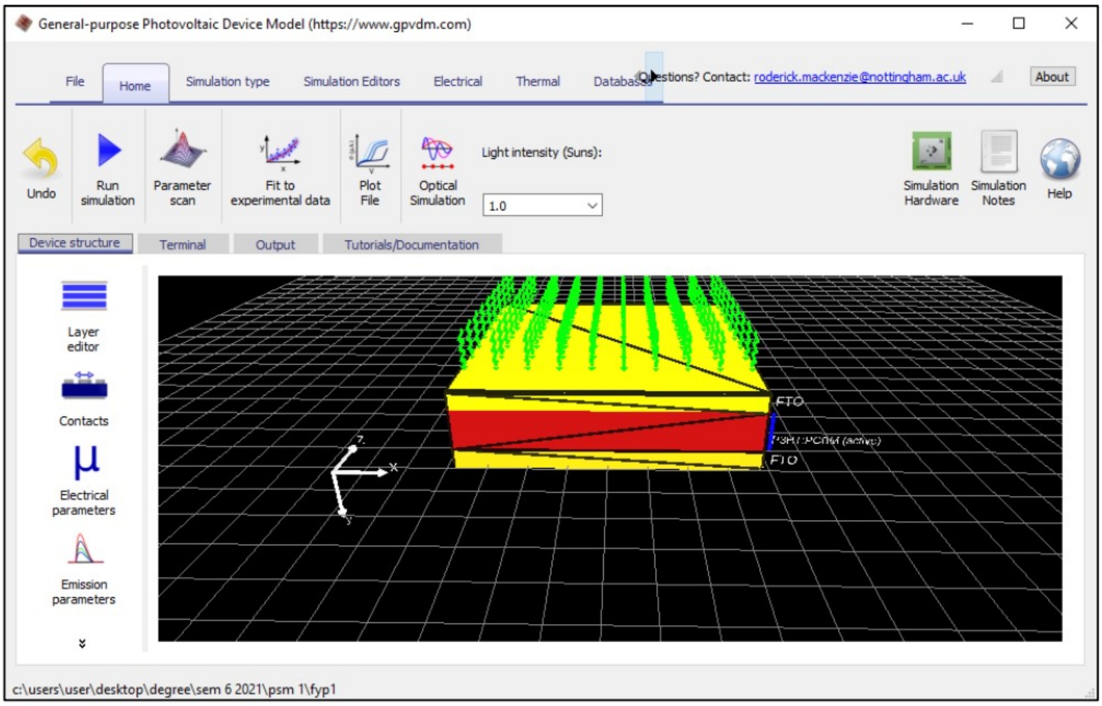

Figure 2.1 The interface of Gpvdm Software

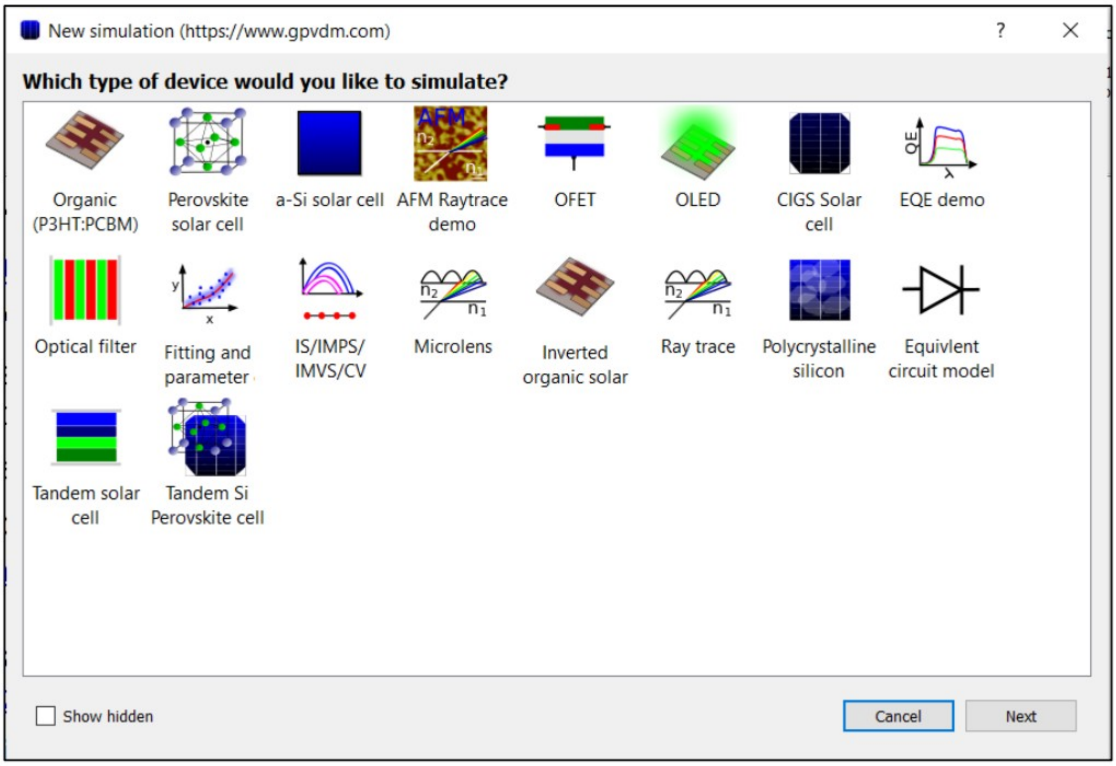

Figure 2.2 Types of Solar Cell in GPVDM Software

CHAPTER 3

METHODOLOGY

3.1 Research Methodology

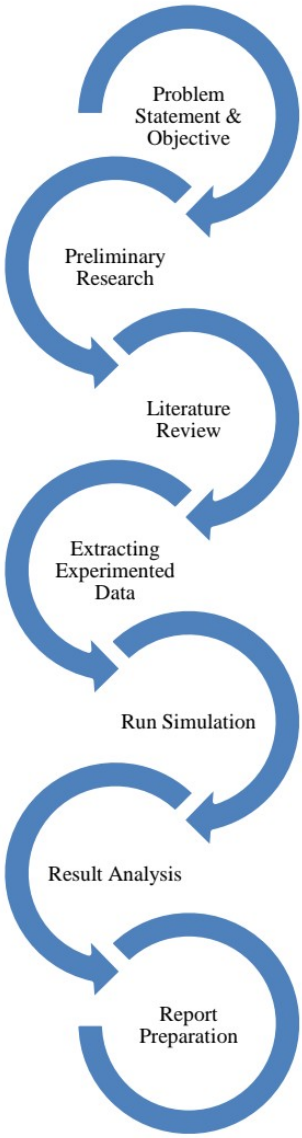

Figure 3.1 Project Methodology

3.2 Electrical Simulation

By computing the electrical field and integrating the absorbed photon distribution throughout the solar spectrum, the transfer matrix approach is utilised to calculate the exciton production rate $G(x)$ inside the active layer. The refractive index $n(\lambda)$ and the extinction coefficient $k(\lambda)$ indicate the optical qualities of each layer. The refractive index is used to calculate the amount of reflected and transmitted light at each interface between two adjacent layers, whereas the extinction coefficient represents a layer's capacity to absorb photons. The following equations indicate the rate of exciton formation.

$$Q(x,\lambda) = \frac{1}{2} c\epsilon_0 \alpha n |E(x)|^2 \quad 3.1$$

$$G(x,\lambda) = \frac{\lambda Q(z,\lambda)}{hc} \quad 3.2$$

$$G(\lambda) = \int_{Solar\ Spectrum} G(x,\lambda) d\lambda \quad 3.3$$

where c is the speed of light, $\alpha = \frac{4\pi k}{\lambda}$ is the absorption coefficient, Q is the energy flow dissipation, E is the electrical field at point x within the material, and h is the plank's constant

For electron and hole currents given by 3.2 to 3.6, the programme employs Poisson's equation, continuity equation, and drift-diffusion equations.

$$\frac{d}{dx}\epsilon_0\epsilon_r\frac{d\phi}{dx} = q(n-p) \quad 3.4$$

$$\frac{\partial J_n}{\partial x} = q\left(R_n - G + \frac{\partial n}{\partial t}\right) \quad 3.5$$

$$\frac{\partial J_p}{\partial x} = -q\left(R_p - G + \frac{\partial p}{\partial t}\right) \quad 3.6$$

$$J_n = q\mu_n\frac{\partial E_c}{\partial x} + qD_n\frac{\partial n}{\partial x} \quad 3.7$$

$$J_p = q\mu_p\frac{\partial E_v}{\partial x} + qD_p\frac{\partial p}{\partial x} \quad 3.8$$

where ϵ_0 and ϵ_r are the free space permittivity and the relative permittivity of the organic blend, ϕ is the voltage profile, x is the dimension perpendicular to the cell surface, J_n and J_p are electron and hole current densities, n and p are electron and hole densities, $R_{n/p}$ is the electron and hole recombination rate, G is the generation rate, and $D_{n/p}$ is the diffusion coefficient.

3.3 Chlorophyll Dye

Below are the 10 sample chlorophyll dyes that are used as photosensitizer in this study. These chlorophylls have been experimented and reported into research paper by previous researchers worldwide.

3.3.1 Neem Leaves

Figure 2 Neem Leaves
Source: Mary Rosana (2015)

Figure 2 shows the Neem or its scientific name is *Azadirachta Indica.* Neem is a famous and widely accessible medicinal tree in India, and all portions of the tree are being studied for biological properties. It has been shown to have anti-inflammatory, antifungal, antibacterial, antioxidant, and other medicinal properties [10].

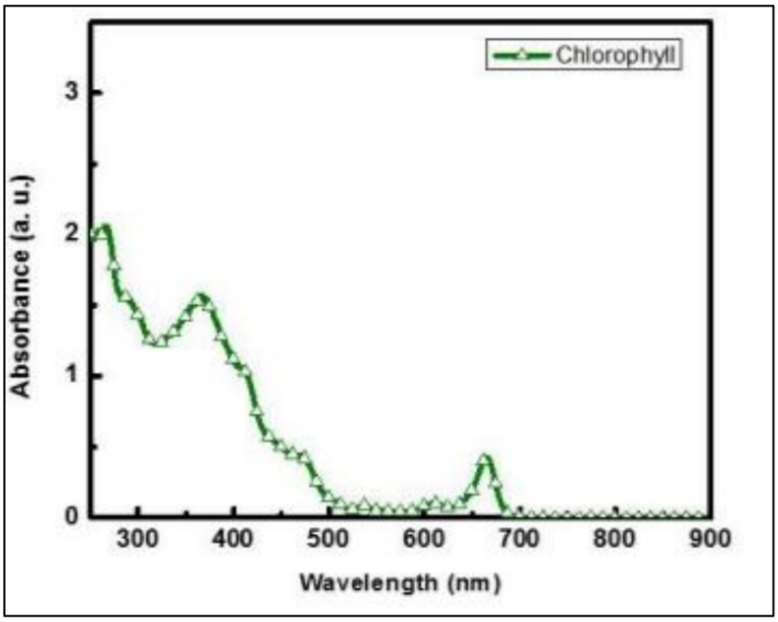

Figure 3 Absorption spectrum of Neem leaves

Source: Mary Rosana (2015)

Figure 3 shows the absorbance data of Neem leaves where it have a wide absorption peak between 300–500 nm and a strong absorption peak between 600-700 nm, with an absorption maximum at 665 nm [10]. The dye is experimented on Fluorine-doped Tin Oxide (FTO) conductive glass where has an active area of 2.25 cm^2 and the research result of current density is shown in Table 1 [10].

Table 1 Research Result of Neem Leaves

Chlorophyll Dye	**Size DSSC (cm^{2})**	**J_{sc} (mA/cm^2)**	**V_{oc} (V)**
Neem Leaves	2.25	0.23	0.467

Source: Mary Rosana et al. (2015)

3.3.2 Apricot Leaves

Apricot or *Prunus Armeniaca* is a deciduous tree that is planted for its tasty fruit. The apricot tree grows upright and has a spreading canopy. The tree's leaves are oval in shape, with a rounded base, pointed tip, and serrated border. Figure 4 below shows the shape of apricot leaves.

Figure 4 Apricot leaves

Source: Internet

Figure 5 shows the absorbance of apricot leaves dye where the extract of apricot exhibited an absorption band at about 394 nm and 3 small bands at 506 nm, 535 nm, and 665 nm [11].

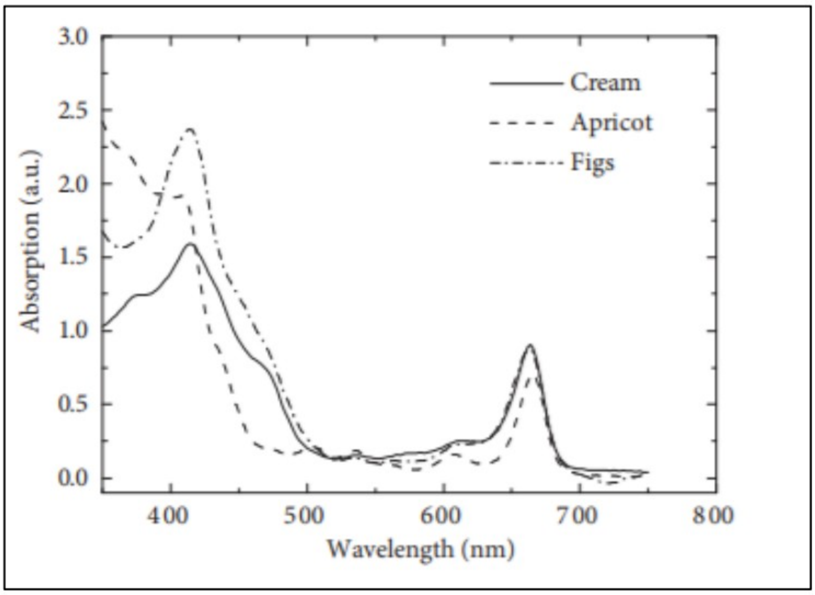

Figure 5 Absorbance Spectra of Apricot Leaves

Source: Taya et al. (2015)

The dye were experimented as photosensitizer on the FTO conductive plates with the size of $1.6\ cm \times 1.6\ cm$ pieces [11]. The result of the experiment was tabulated in the Table 2 below.

Table 2 Research Result of Apricot Leaves Dye

Chlorophyll Dye	Area DSSC (cm^2)	J_{sc} (mA/cm^2)	V_{oc} (V)
Apricot Leaves	2.56	0.771	0.620

Source: Taya et al. (2015)

3.3.3 Papaya Leaves

Carica papaya, usually known simply as papaya, is a tropical, fruit-bearing tree. Today, papaya is one of the world's most frequently produced crops. Its fruit, seeds, and leaves are widely used in culinary and folk medical traditions. In test-tube and animal experiments, papaya leaf includes unique plant chemicals that have proven broad pharmacological potential [12].

Figure 6 Papaya leaf

Source: Internet

Figure 7 shows the absorbance data of the Papaya leaves where it has absorption peak at 460-500 nm.

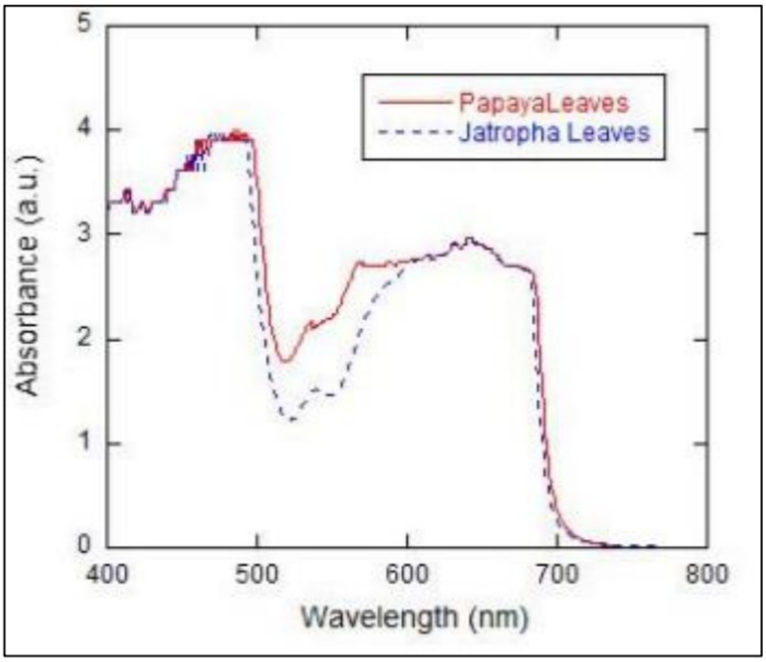

Figure 7 Absorption Spectra of Papaya Leaves
Source: Pramono et al. (2015)

The dye were experimented as photosensitizer on the Indium Tin Oxide (ITO) conductive plates with the size of 2 cm × 2 cm pieces [12]. The result of the experiment was tabulated in the Table 3 below.

Table 3 Research Result of Papaya Leaves Dye

Chlorophyll Dye	**Area DSSC (cm^2)**	**J_{sc} (mA/cm^2)**	**V_{oc} (V)**
Papaya Leaves	4	0.060	0.394

Source: Pramono et al. (2015)

3.3.4 Pawpaw Leaves

The fruit of the *Asimina triloba* tree, which is endemic to the eastern United States and southern Canada, is pawpaw. They have a sweet, tropical flavour and are the biggest edible fruit native to North America. Figure 8 shows the shape of Pawpaw leaves.

Figure 8 Pawpaw Leaves
Source: Internet

Figure 9 depicts the absorption spectra of pawpaw leaf dye, with an absorbability range of 350 - 500 nm and an absorption peak at 430 nm [13].

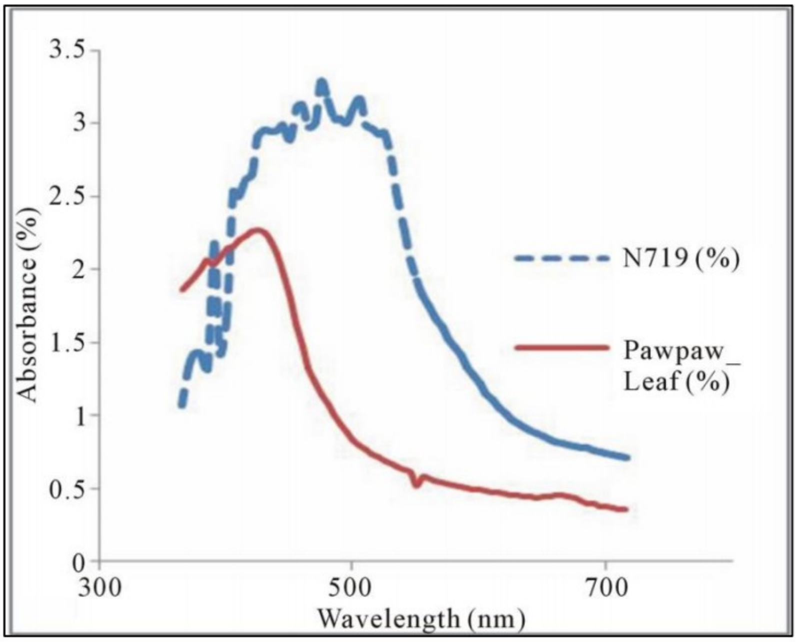

Figure 9 Absorption Spectrum of Pawpaw Leaves
Source: Isah Kimpa et al. (2012)

The pawpaw leaves dye is experimented on FTO conductive glass where has an active area of 0.54 cm^2 which is 1.4 cm × 0.39 cm [13]. The experimented result of J_{sc} and V_{oc} is tabulated in the Table 4 below.

Table 4 Research Result of Pawpaw Leaves Dye

Chlorophyll Dye	Area DSSC (cm^2)	J_{sc} (mA/cm^2)	V_{oc} (V)
Pawpaw Leaves	0.54	0.649	0.504

Source: Isah Kimpa et al. (2012)

3.3.5 Scent Leaves

The scent leaf, botanically known as *Ocimum gratissimum*, is a fragrant herb that has been widely disseminated across the world's tropical and subtropical climates. Scent leaf is indigenous to Nigeria, Ghana, and areas of Africa and Asia. This is a homegrown shrub that is commonly found in farm and garden settings and is mostly utilised as a spice in culinary delicacies owing to its fragrant flavour [14]. Figure 10 shows the shape of Scent leaves

Figure 10 Scent leaves

Source: Internet

Figure 11 shows the absorption spectra of the Scent leaves dye (purple colour line) which has a peak at 390 nm [14].

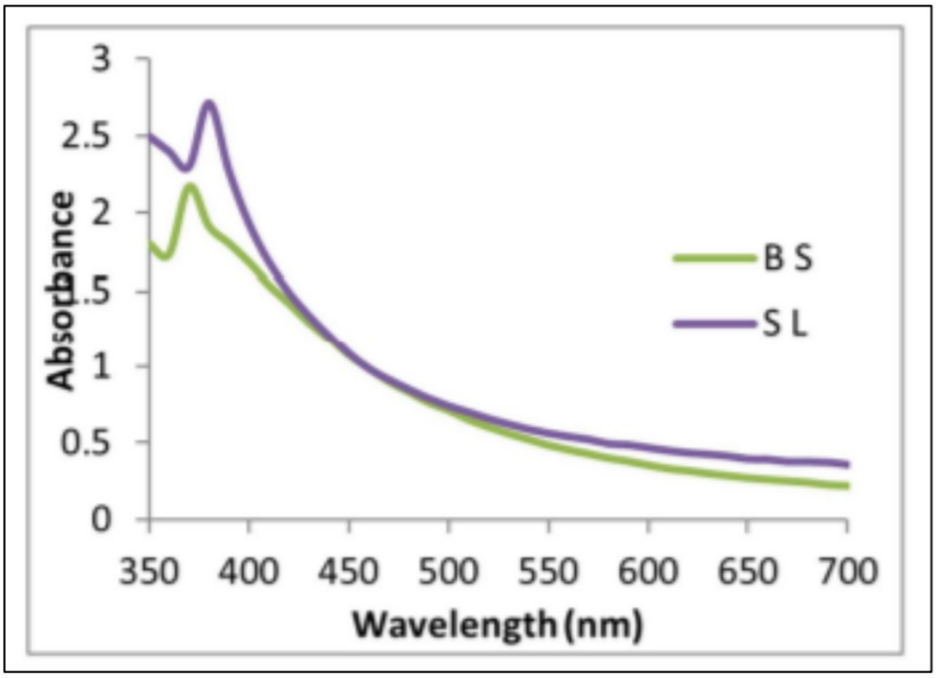

Figure 11 Absorption Spectra of Scent Leaves Dye

Source: Eli (2016)

The scent leaves dye is experimented on FTO conductive glass and the experimented result of J_{sc} and V_{oc} is tabulated in the Table 5 below.

Table 5 Research Result of Scent Leaves Dye

Chlorophyll Dye	**Area DSSC (cm^2)**	**J_{sc} (mA/cm^2)**	**V_{oc} (V)**
Scent Leaves	Assumed 1	0.044	0.466

Source: Eli (2016)

3.3.6 Spinach

Spinach with scientific name *Spinacia Oleracea* is the most well-known of the edible leaves known as 'greens,' which also include dandelion, mustard, beet tops, and turnip tops. Spinach is planted as an early spring and late fall crop to ensure growth throughout the coldest sections of the season. Spinach grown under warm weather becomes fibrous and rough and instead of the regular flavour, it is fairly harsh and unpalatable.

Figure 12 Spinach

Source: Internet

Figure 13 shows the UV-VIS absorption spectra for the extracts of spinach (A) with the absorption peak at 701 nm [15].

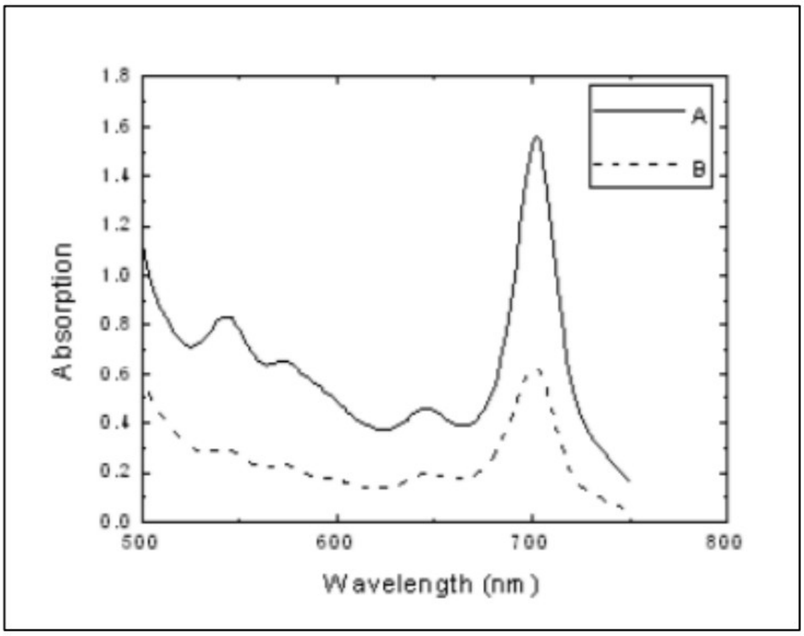

Figure 13 Absorption Spectra of Spinach (A)

Source: Taya (2013)

The spinach dye is experimented on FTO conductive glass where has an active area of 0.25 cm^2. The experimented result of J_{sc} and V_{oc} is tabulated in the Table 6 below.

Table 6 Research Result of Spinach Dye

Chlorophyll Dye	Area DSSC (cm^2)	J_{sc} (mA/cm^2)	V_{oc} (V)
Spinach	0.25	1.11	0.583

Source: Taya (2013)

3.3.7 Ti Plant Leaves

Cordyline fruticosa is a flowering plant of the *Asparagaceae* family. The plant is extremely important in the old animistic religions of the Pacific Islands, New Zealand, Island Southeast Asia, and Papua New Guinea's Austronesian and Papuan peoples [16]. It is also used for food, traditional medicine, and as a decorative due to its multicoloured leaves. It is known by several other names, including ti plant, palm lily, and cabbage palm [16]. Figure 14 below shows the shape of Ti plant leaves.

Figure 14 Ti Plant Leaves
Source: Internet

The absorption spectra of Ti plant leaves extracts (purple colour line) is shown in Figure 15. The extract has a noticeable absorption spectrum between 630 and 700 nm. At 530, 605, and 660 nm, three major peaks were discovered. The figure also depicts large absorption bands ranging from 470 to 570 nm [16].

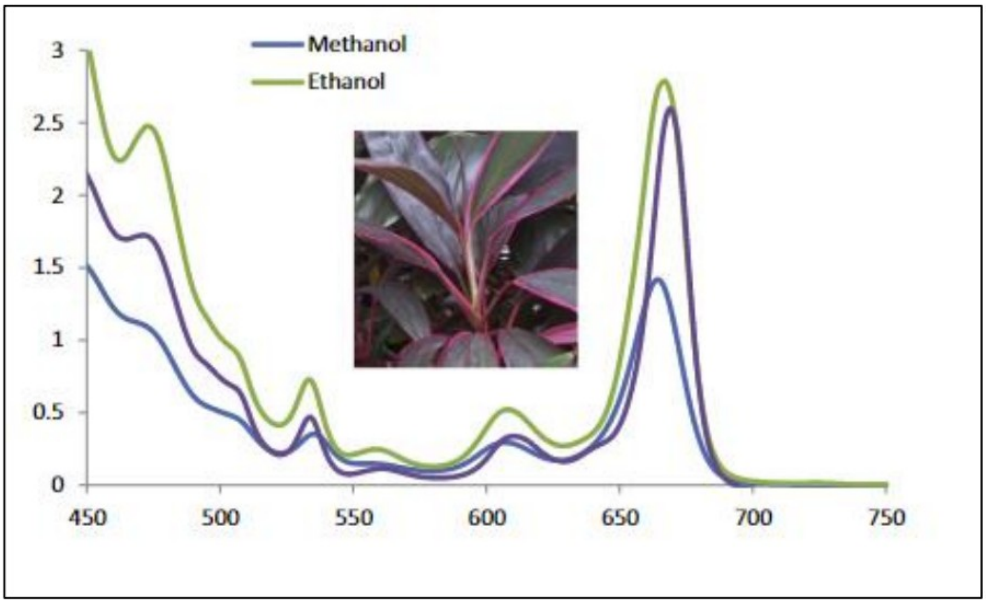

Figure 15 Absorption Spectra of Ti Plant Leaves (Purple Line)
Source: Al-Alwani et al. (2016)

The Ti plant dye is experimented on FTO conductive glass where has an active area of 1 cm^2 [16]. The experimented result of J_{sc} and V_{oc} is tabulated in the Table 7 below.

Table 7 Research Result of Ti Plant Leaves Dye

Chlorophyll Dye	**Area DSSC (cm^2)**	**J_{sc} (mA/cm^2)**	**V_{oc} (V)**
Ti Plant Leaves	1	1.3	0.616

Source: Al-Alwani et al. (2016)

3.3.8 Morning Glory Leaves

Morning glory or *Ipomoea Purpurea* are an annual vining flower that bloom early in the day. They are plants that enjoy climbing [17]. Their blooms are brilliant in purple, blue, red, pink, and white, with the heart-shaped leaf as shown in Figure 16 attracting hummingbirds and butterflies.

Figure 16 Morning Glory Leaves
Source: Internet

The absorption spectra of Morning Glory leaf extract following UV irradiation are shown in Figure 17. According to the spectra curves, the greatest absorption peak value of ipomoea extract fluid is at 410 nm [17].

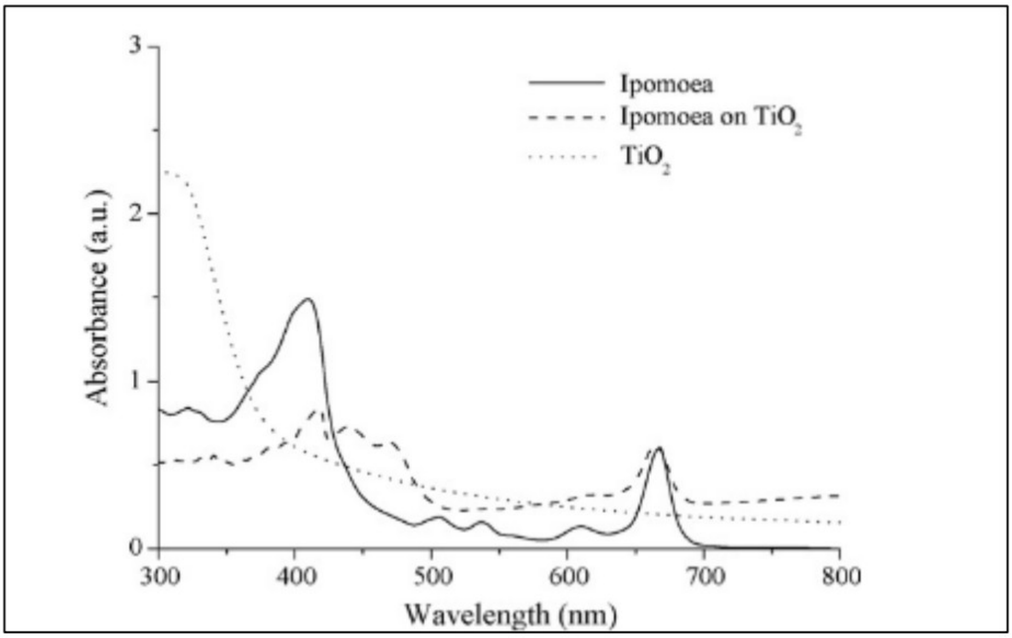

Figure 17 Absorption Spectra of Morning Glory Leaves
Source: Chang et al. (2010)

The Morning Glory leaves dye is experimented on ITO conductive glass where has an active area of 0.25 cm^2 [17]. The experimented result of J_{sc} and V_{oc} is tabulated in the Table 8 below.

Table 8 Research Result of Morning Glory Leaves Dye

Chlorophyll Dye	**Area DSSC (cm^2)**	**J_{sc} (mA/cm^2)**	**V_{oc} (V)**
Morning Glory Leaves	0.25	0.85	0.495

Source: Chang et al. (2010)

3.3.9 Jatropha Curcas Leaves

Jatropha curcas with scientific name *Euphorbiaceae* is a spurge-like flowering plant endemic to the American tropics, most likely Mexico and Central America. It originates originated from the tropical sections of the Americas, from Mexico to Argentina, and has spread around the world in tropical and subtropical climates, becoming naturalised or invasive in many places. It is a multipurpose plant with the potential to produce biodiesel and be used medicinally [12]. It has been used to treat a wide range of disorders including skin, cancer, digestive, respiratory, and infectious diseases. Figure 18 shows the shape of Jatropha Curcas leaves.

Figure 18 Jatropha Curcas Leaves
Source: Internet

Figure 19 shows the absorbance spectra of the Jatropha Curcas leaves where it has absorption peak at 460-500 nm.

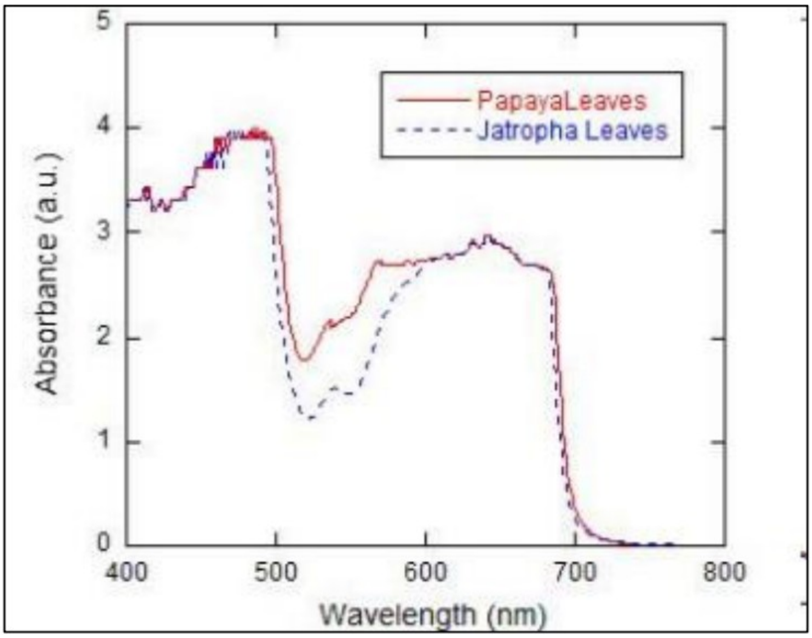

Figure 19 Absorption Spectra of Jatropha Curcas Leaves

Source: Pramono et al. (2015)

The dye were experimented as photosensitizer on the ITO conductive plates with the size of 2 cm × 2 cm pieces [12]. The result of the experiment was tabulated in the Table 9 below.

Table 9 Research Result of Jatropha Curcas Leaves Dye

Chlorophyll Dye	**Area DSSC (cm^2)**	**J_{sc} (mA/cm^2)**	**V_{oc} (V)**
Jatropha Carcus Leaves	4	0.042	0.35

Source: Pramono et al. (2015)

3.3.10 Chinar Leaves

Chinar or *Platanus Orientalis* is a tall, deciduous tree of the Platanaceae family that may grow to 30 m (98 ft) or more in height and is notable for its longevity and spreading crown. Its rich green foliage become blood crimson, amber, and yellow in the fall [18]. The leaves and bark have been utilised for therapeutic purposes. The twigs and roots have been used to create a fabric dye. The wood, sometimes known as lacewood, is figured and valued for interior furniture. Artists frequently utilise the leaves for leaf carving [18]. Figure 20 shows the shape of Chinar leaves.

Figure 20 Chinar Leaves

Source: Internet

Figure 21 shows the UV-VIS absorption spectra for the extracts of Chinar leaves (a), the red line with the absorption peak at 445 nm.

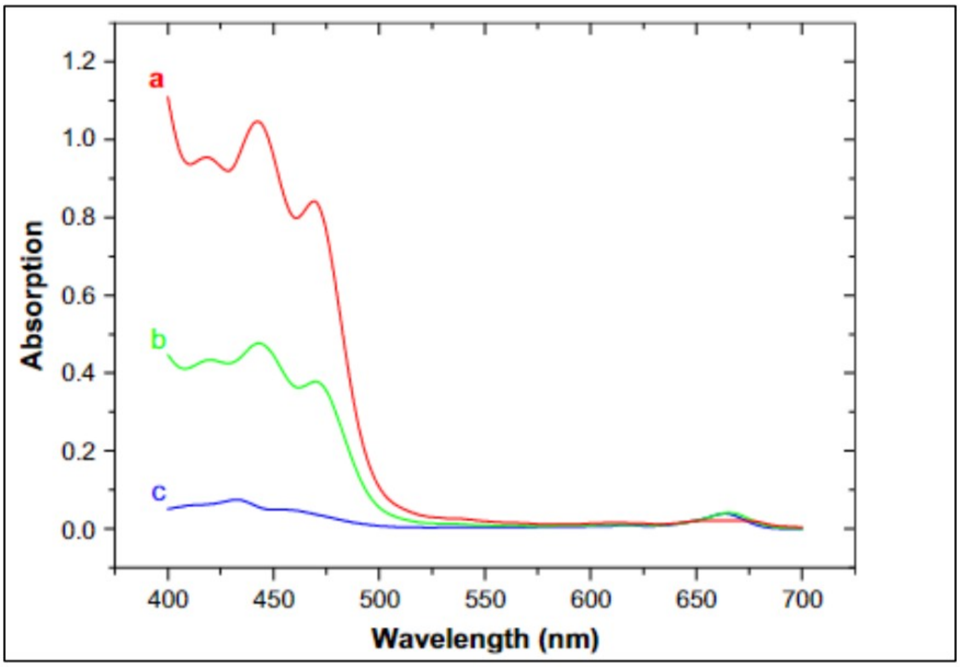

Figure 21 Absorption Spectra of Chinar Leaves Dye (a)

Source: Liu et al. (2008)

The dye was experimented as photosensitizer on the ITO conductive plates with the size of 2.5 cm × 2.5 cm pieces [18]. The result of the experiment was tabulated in the Table 10 below.

Table 10 Research Result of Chinar Leaves Dye

Chlorophyll Dye	Area DSSC (cm^2)	J_{sc} (mA/cm^2)	V_{oc} (V)
Chinar Leaves	6.25	0.012	0.468

Source: Liu et al. (2008)

3.4 Inserting Data for New Material

When the new material needs to be inserted into GPVDM software, the absorbance data and refractive index data are needed in order to run the simulation in it. For this study, all 10 samples chlorophyll dye are inserted into GPVDM because the software does not have any data about the materials. Since the related data need to be acquired first, it is extracted from the previous research paper that have been experimenting the chlorophyll dyes.

Most of the research paper only shows the graph of absorption spectra which is same as absorbance of the material. So, in order to extract the data from, the WebPlotDigitizer is used to get the data from the graph. The WebPlotDigitizer can be use directly from its website or download the software. Figure 22 below shows the interface of the software.

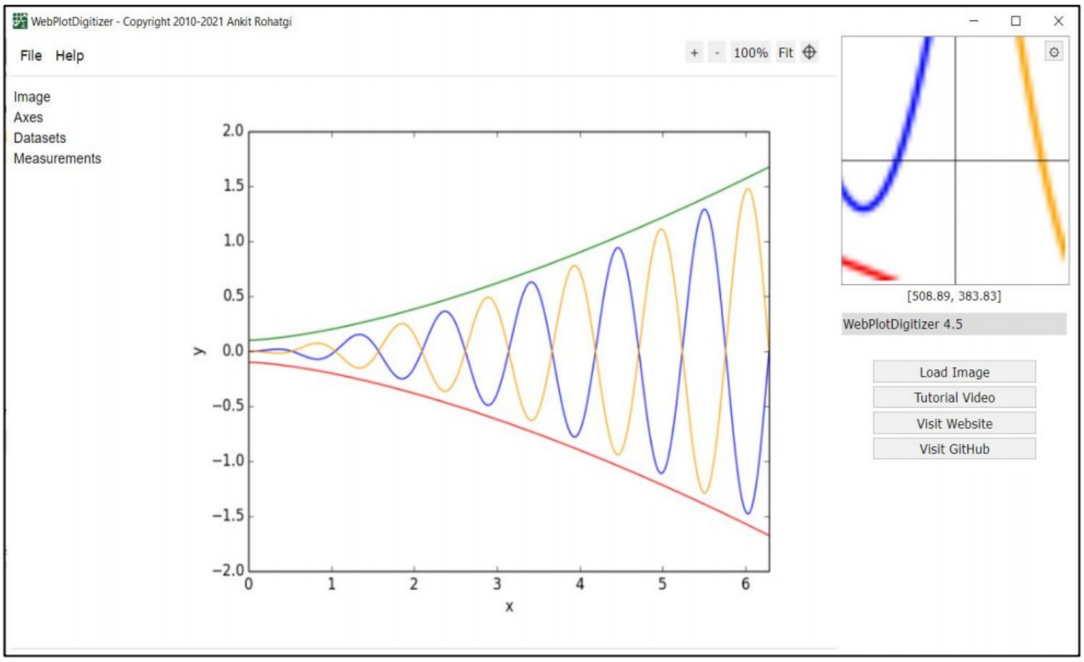

Figure 22 Interface of WebPlotDigitizer

After that, insert or load in the image of graph that need to be extracted the data into the WebPlotDigitizer. Figure 23 below shows an example of graph that have been uploaded.

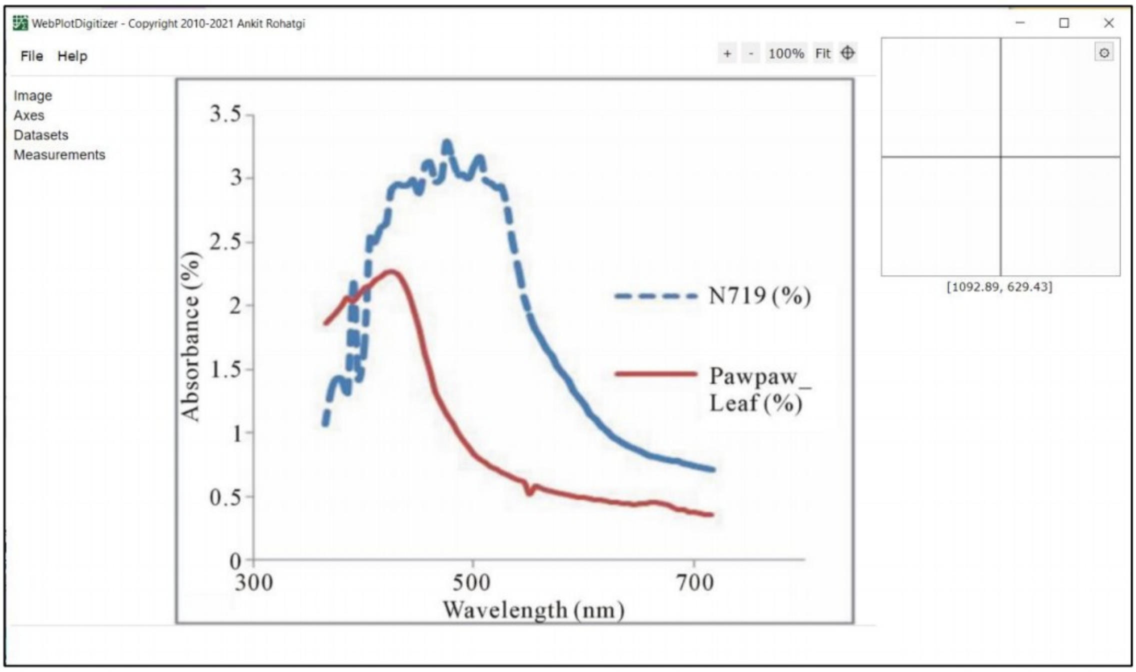

Figure 23 Loaded Image inside the WebPlotDigitizer

Then, the needed graph need to be drawn as shown in the Figure 24 below.

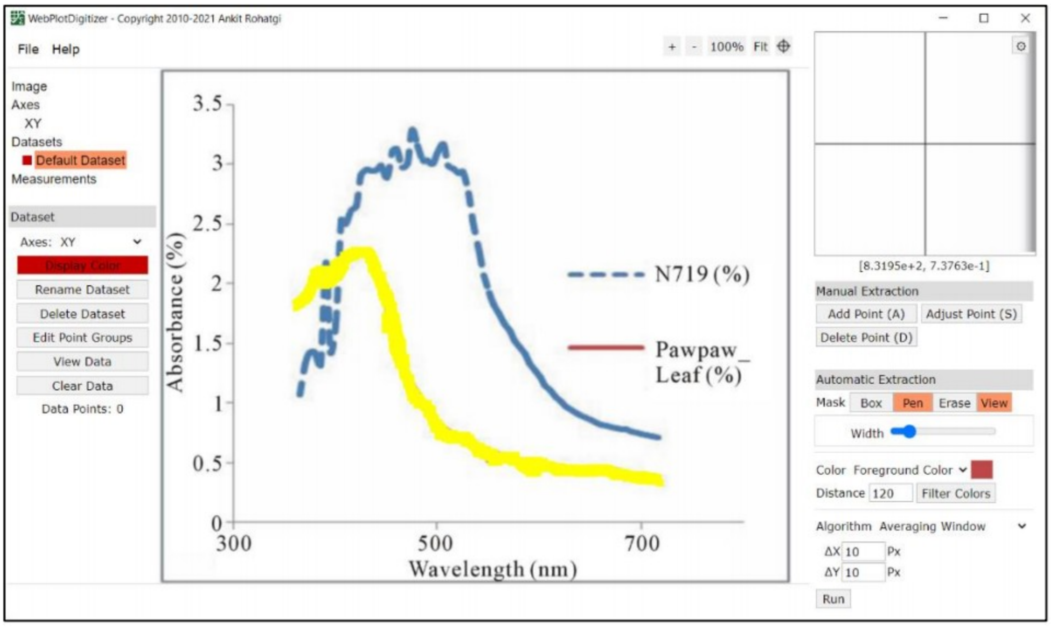

Figure 24 Draw the Graph Needed in WebPlotDigitizer

After the graph has been drawn, the software is simulated to get the plot on the graph that have been drawn as shown in Figure 25.

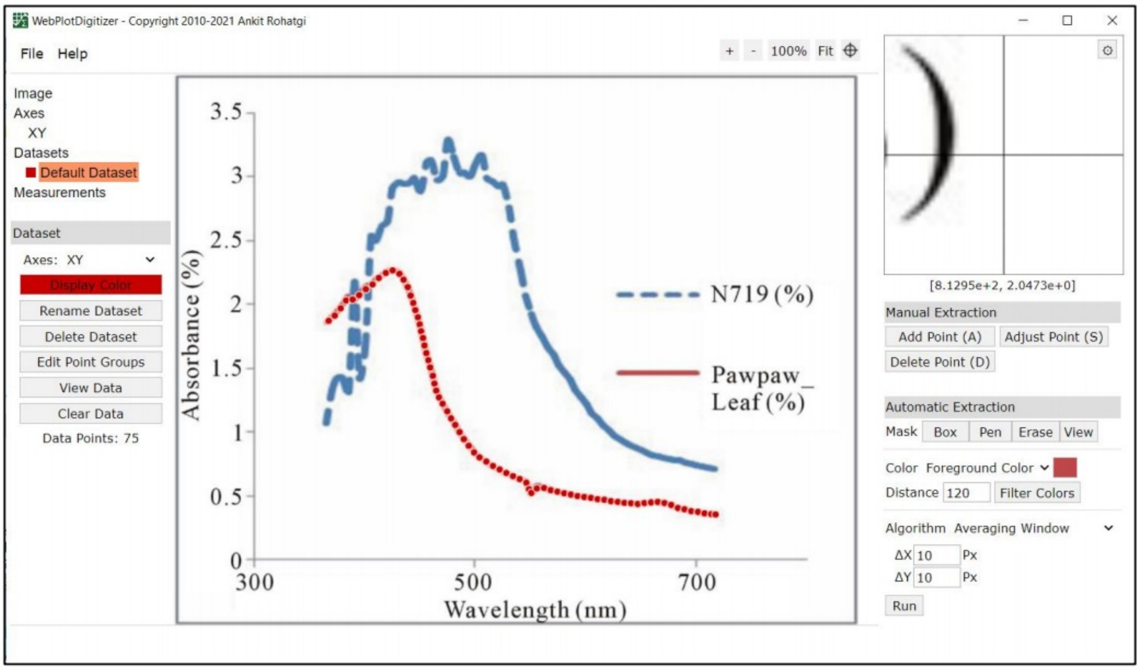

Figure 25 Plot on the Graph in WebPlotDigitizer

After plotting the graph, the data of the graph can be view as shown below in Figure 26, where this is the type of data that is needed in the GPVDM software.

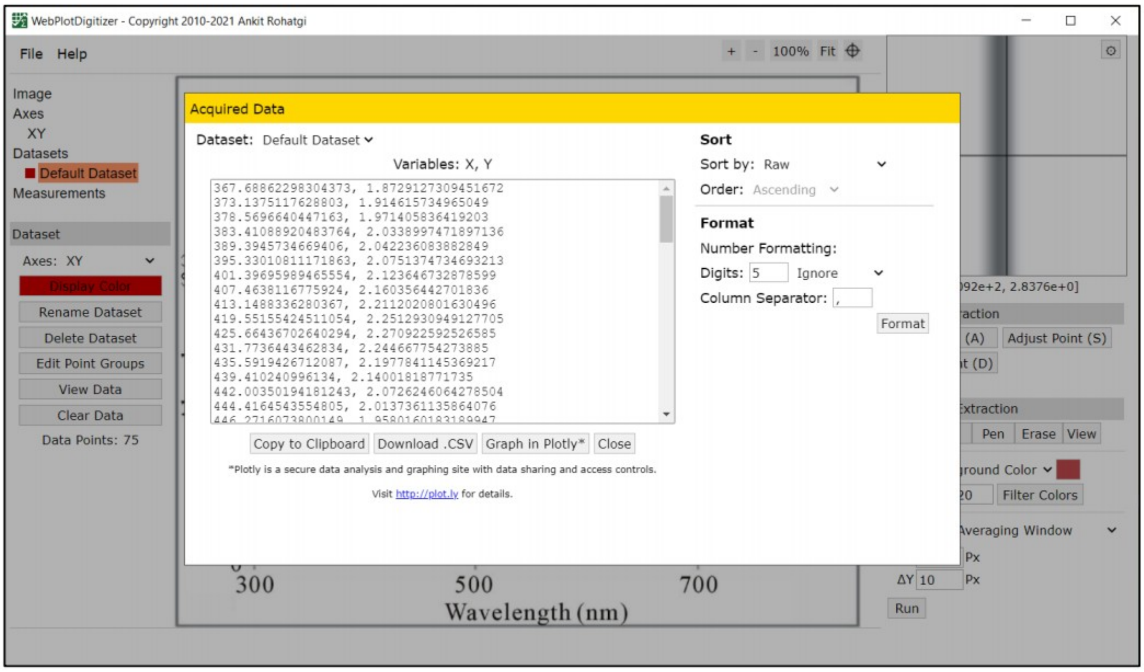

Figure 26 Data of The Plotted Graph

After acquiring the data needed, the file of data is imported into GPVDM software as shown in Figure 27 and then, the GPVDM software will automatically construct the graph from the data file.

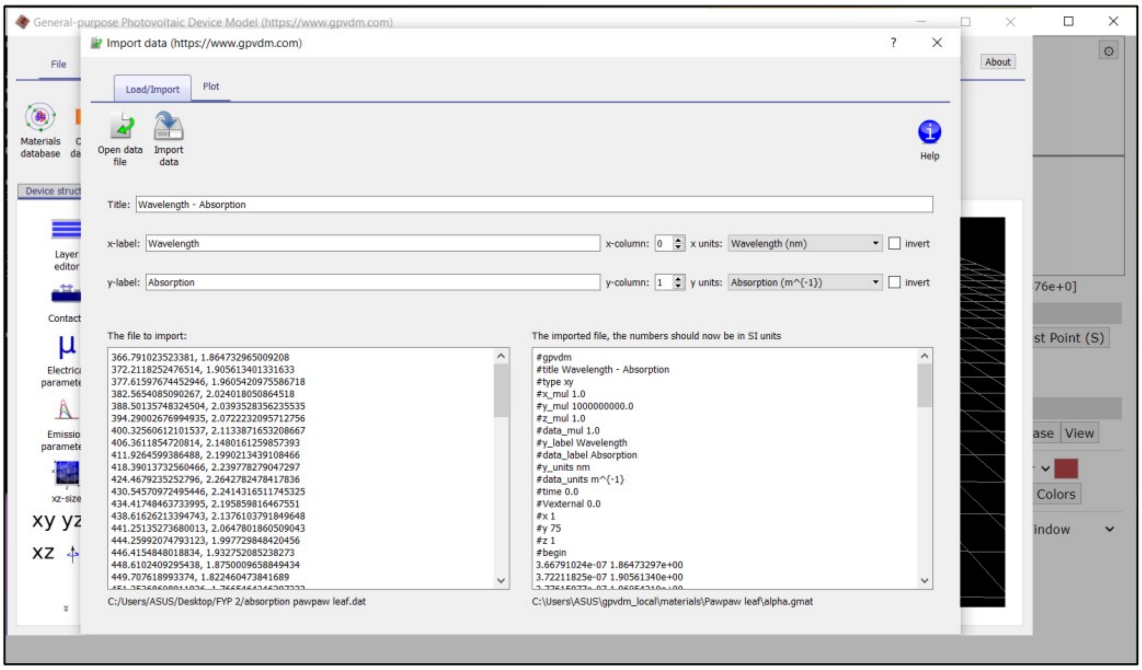

Figure 27 Data of Graph is Imported into GPVDM Software

3.5 Simulation of DSSC

The device structure is divided into several layers of various materials. These may be set up via the layer editor. Some of these layers will be of the active variety that will be subjected to the electrical model. For this study, the chlorophyll-dye layer is set as an active layer. To function, the electrical model requires a finite difference mesh to be built up. Typically, GPVDM will handle this automatically. For this study, the default electrical parameter in the software is used because most of the research paper does not mentioning or stated the electrical parameter of the chlorophyll. Figure 28 shows the electrical parameter that have been used for this study.

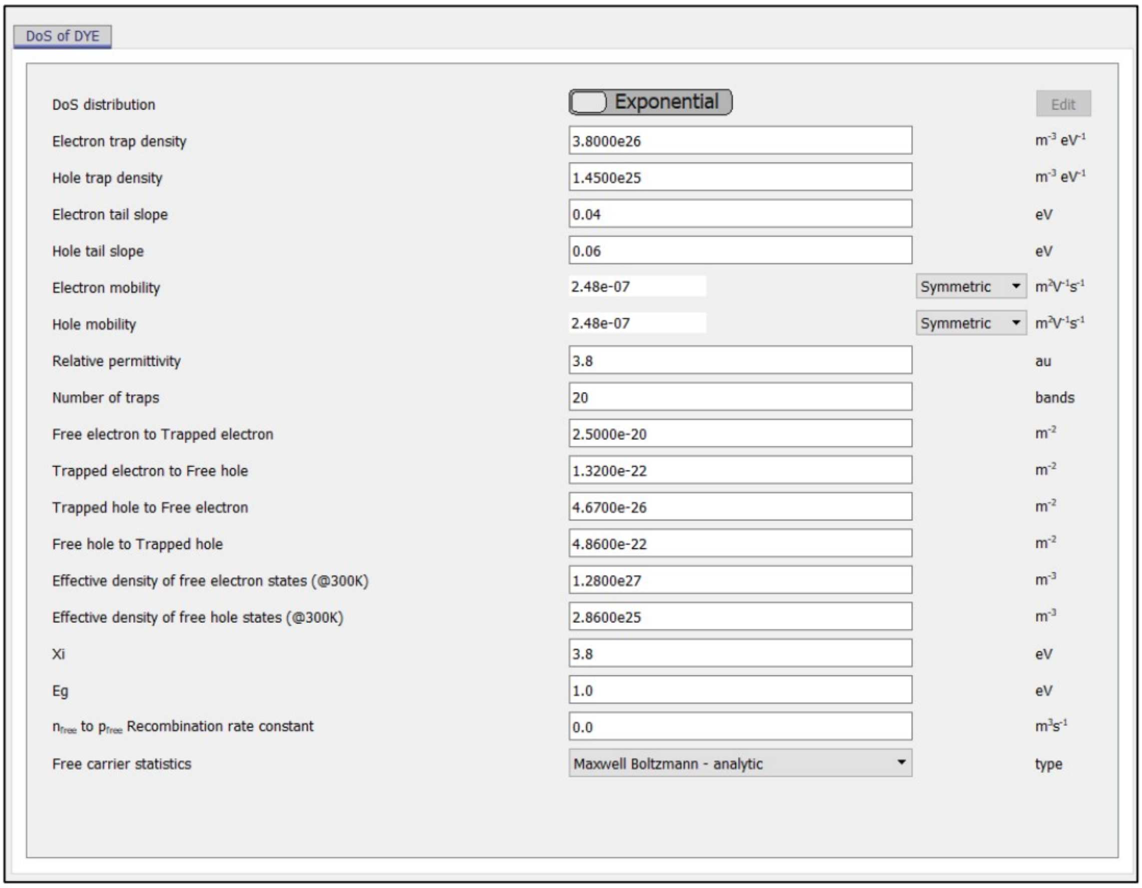

Figure 28 Electrical Parameter Used For Simulation

The simulation follows the exact size of active area DSSC that have been researched in previous research paper. Different types of chlorophyll dye are experimented on different size of conductive glass. Figure 4.1 shows the section to manipulate the size of DSSC in GPVDM software so that it can follow the size that have been mentioned in research paper according to the type of chlorophyll dye.

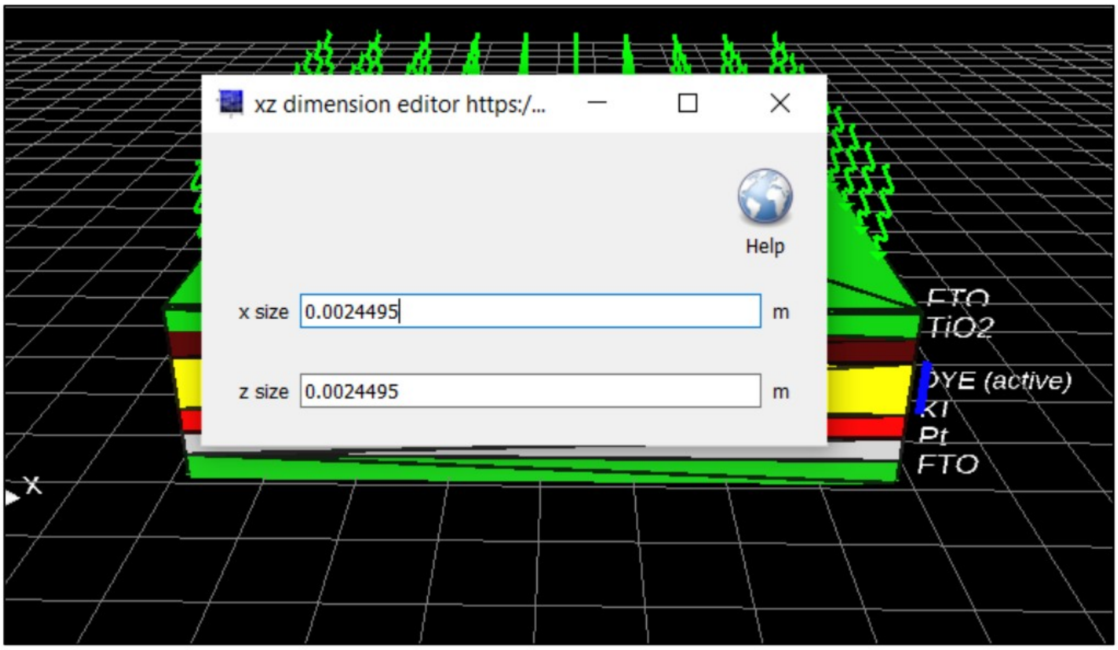

Figure 29 Section to Change Size of DSSC in GPVDM

3.6 Gantt chart

A gantt chart was created to maintain the project's consistency by ensuring that the objective was met at the specified time. This gantt chart will also be used as a rough guide. In the Appendix A section, there is a gantt chart during this semester.

CHAPTER 4

RESULTS AND DISCUSSION

4.1 Result Simulation

The result of simulation of J-V curve for all 10 chlorophyll dyes is shown below and the value for simulation of I_{sc}, J_{sc} and V_{oc} also tabulated below. The simulation follows the area of DSSC that have been mentioned in the related research paper, while for the size area of DSSC that are not been mentioned is assumed by 1 cm^2.

4.1.1 Neem Leaves

Figure 30 and 31 show I-V curve and J-V curve of simulation using Neem leaves as dye respectively. The value for I_{sc}, J_{sc} and V_{oc} is tabulated in Table 11.

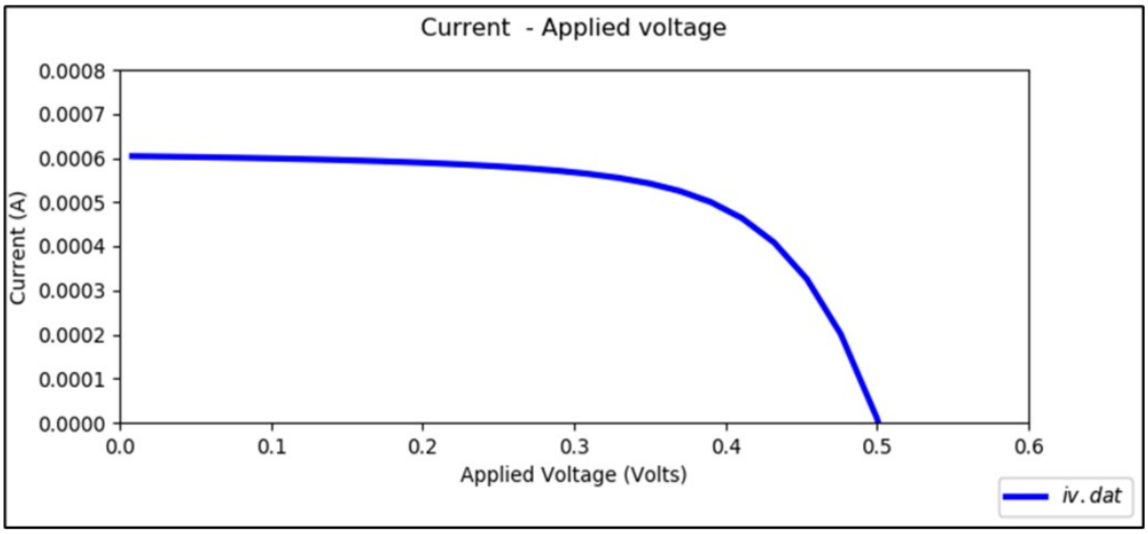

Figure 30 I-V Curve for Neem Leaves Dye

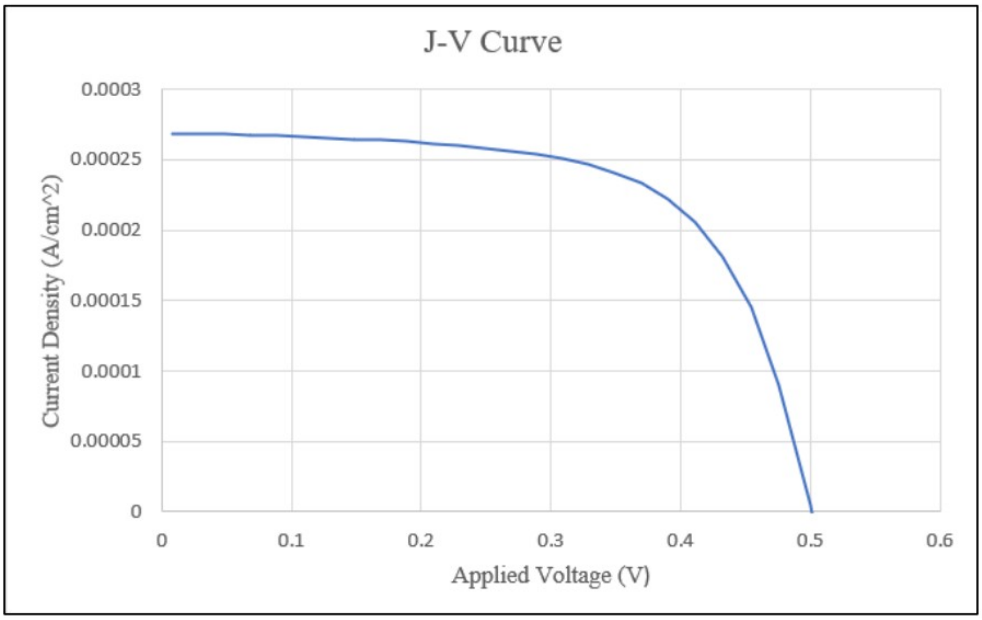

Figure 31 J-V Curve for Neem Leaves Dye

Table 11 Simulation Result for Neem Leaves Dye

Chlorophyll Dye	Area DSSC (cm^2)	I_{sc} (mA)	J_{sc} (mA/cm^2)	V_{oc} (V)
Neem Leaves	2.25	0.6	0.2667	0.5

4.1.2 Apricot Leaves

Figure 32 and 33 show I-V curve and J-V curve of simulation using Apricot leaves as dye respectively. The value for Isc, Jsc and Voc is tabulated in Table 12.

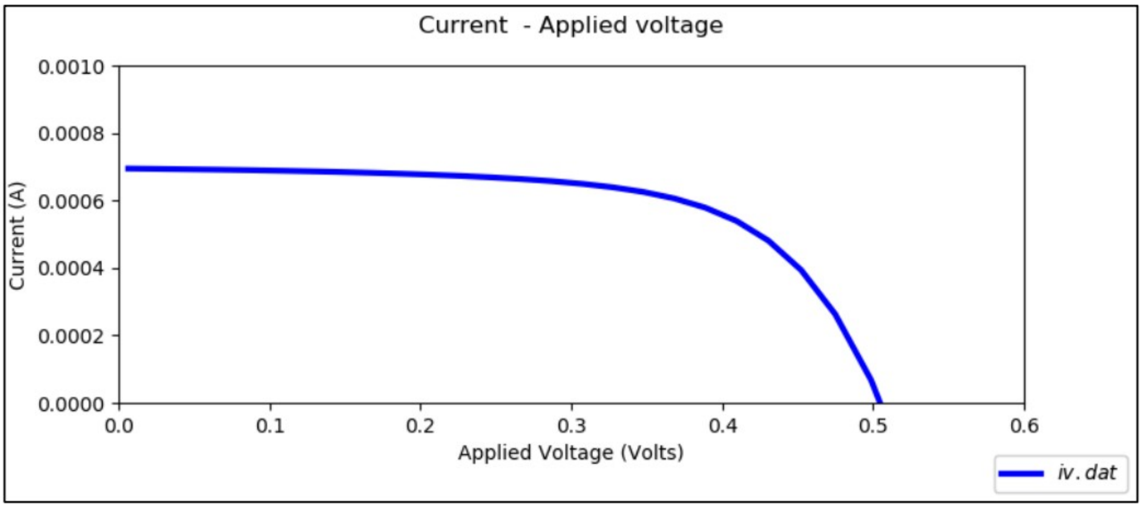

Figure 32 I-V Curve for Apricot Leaves Dye

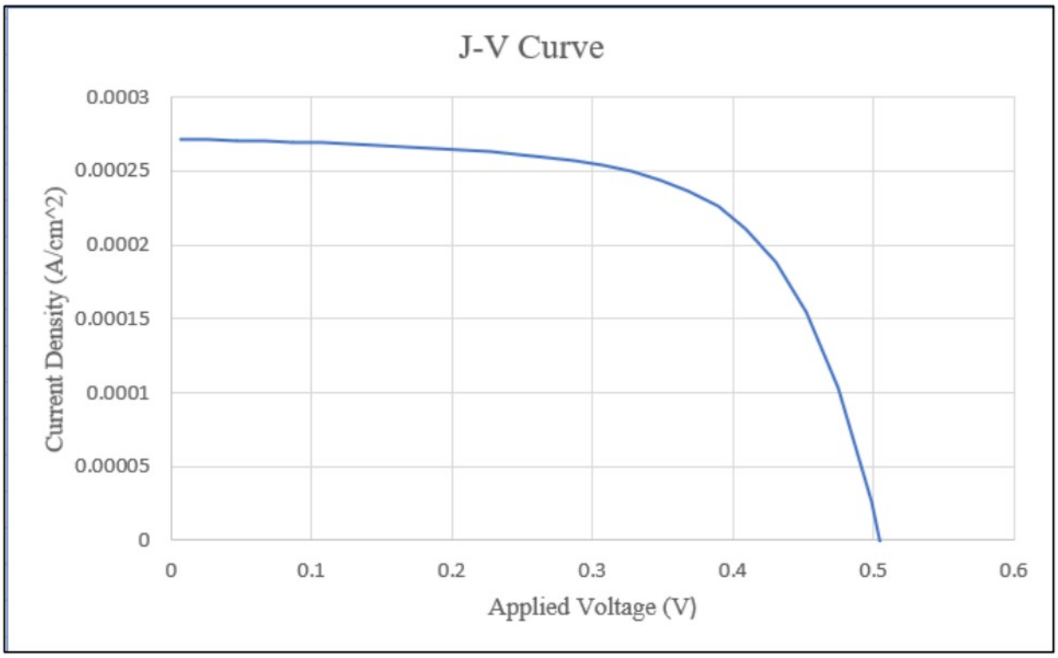

Figure 33 J-V Curve for Apricot Leaves Dye

Table 12 Simulation Result for Apricot Leaves Dye

Chlorophyll Dye	Area DSSC (cm^2)	I_{sc} (mA)	J_{sc} (mA/cm^2)	V_{oc} (V)
Apricot Leaves	2.56	0.695	0.271	0.524

4.1.3 Papaya Leaves

Figure 34 and 35 show I-V curve and J-V curve of simulation using Apricot leaves as dye respectively. The value for Isc, Jsc and Voc is tabulated in Table 13.

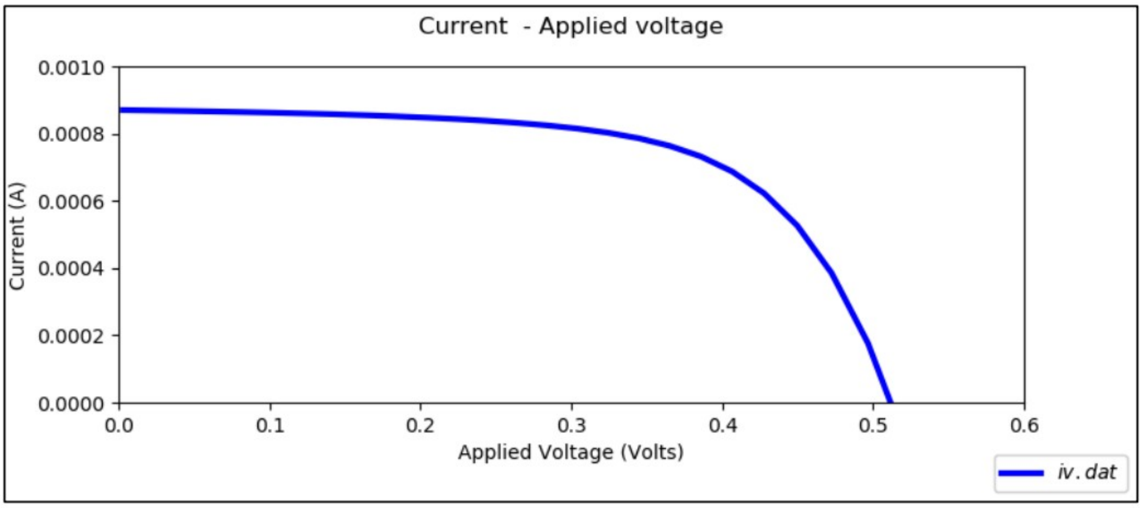

Figure 34 I-V Curve for Papaya Leaves Dye

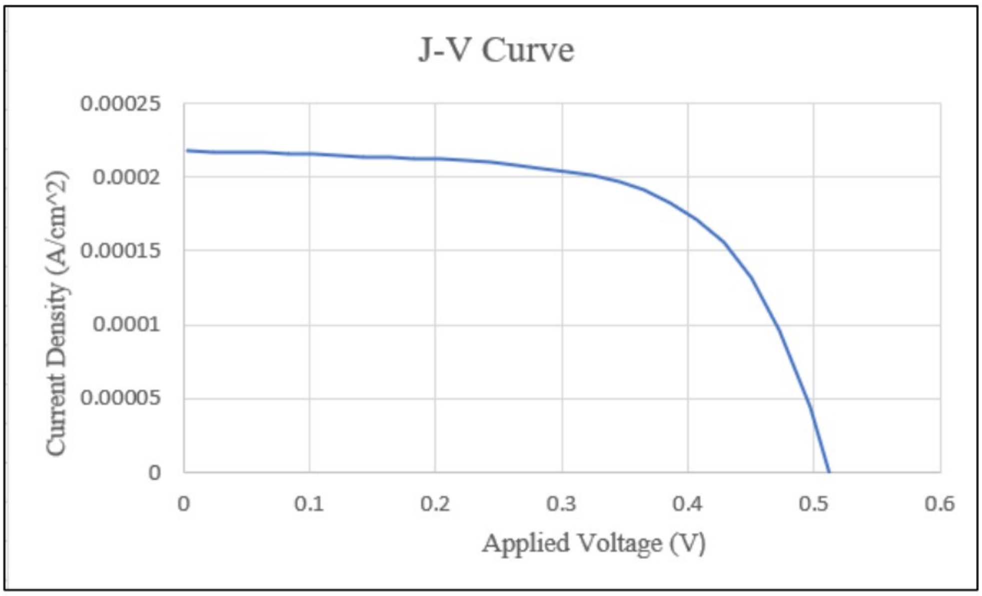

Figure 35 J-V Curve for Papaya Leaves Dye

Table 13 Simulation Result for Papaya Leaves Dye

Chlorophyll Dye	Area DSSC (cm^2)	I_{sc} (mA)	J_{sc} (mA/cm^2)	V_{oc} (V)
Papaya Leaves	4	0.87	0.2175	0.523

4.1.4 Pawpaw Leaves

Figure 36 and 37 show I-V curve and J-V curve of simulation using Pawpaw leaves as dye respectively. The value for Isc, Jsc and Voc is tabulated in Table 14.

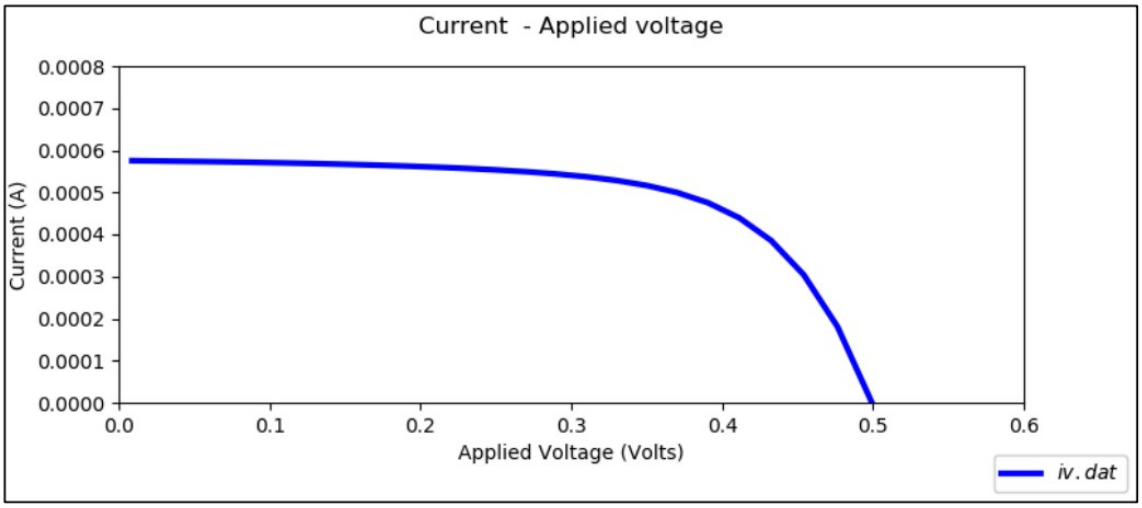

Figure 36 I-V Curve for Pawpaw Leaves Dye

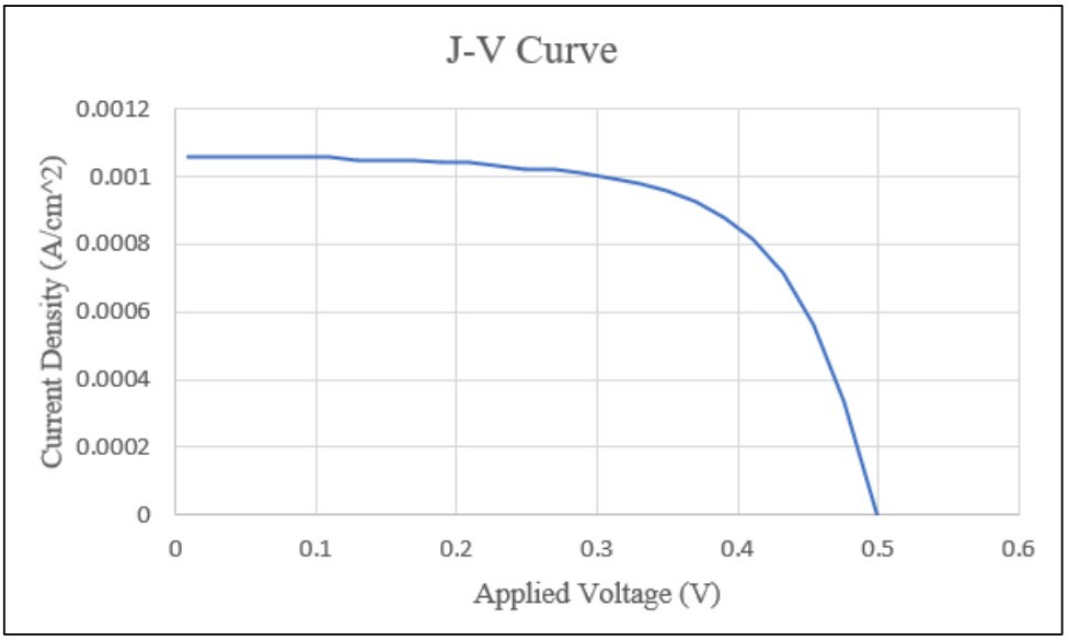

Figure 37 J-V Curve for Pawpaw Leaves Dye

Table 14 Simulation Result for Pawpaw Leaves Dye

Chlorophyll Dye	**Area DSSC (cm^2)**	**I_{sc} (mA)**	**J_{sc} (mA/cm^2)**	**V_{oc} (V)**
Pawpaw Leaves	0.54	0.575	1.0648	0.5

4.1.5 Scent Leaves

Figure 38 and 39 show I-V curve and J-V curve of simulation using Scent leaves as dye respectively. The value for Isc, Jsc and Voc is tabulated in Table 15.

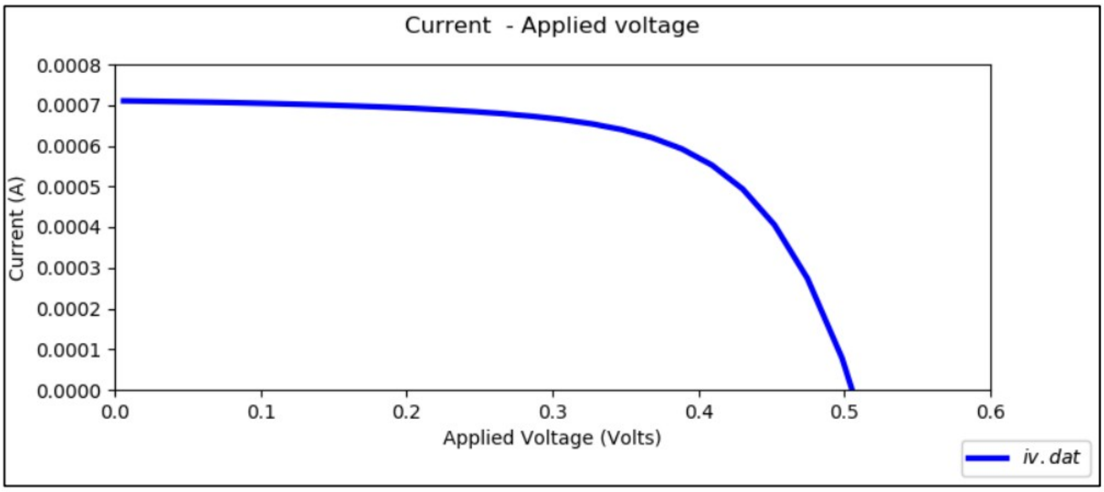

Figure 38 I-V Curve for Scent Leaves Dye

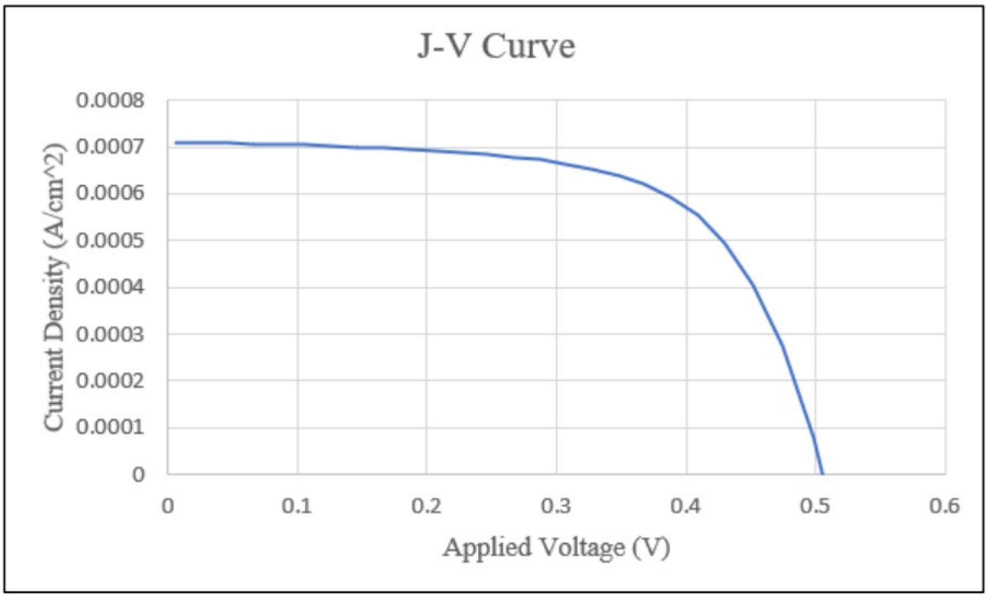

Figure 39 J-V Curve for Scent Leaves Dye

Table 15 Simulation Result for Scent Leaves Dye

Chlorophyll Dye	**Area DSSC (cm^2)**	**I_{sc} (mA)**	**J_{sc} (mA/cm^2)**	**V_{oc} (V)**
Scent Leaves	1	0.71	0.71	0.524

4.1.6 Spinach

Figure 40 and 41 show I-V curve and J-V curve of simulation using Spinach as dye respectively. The value for Isc, Jsc and Voc is tabulated in Table 16.

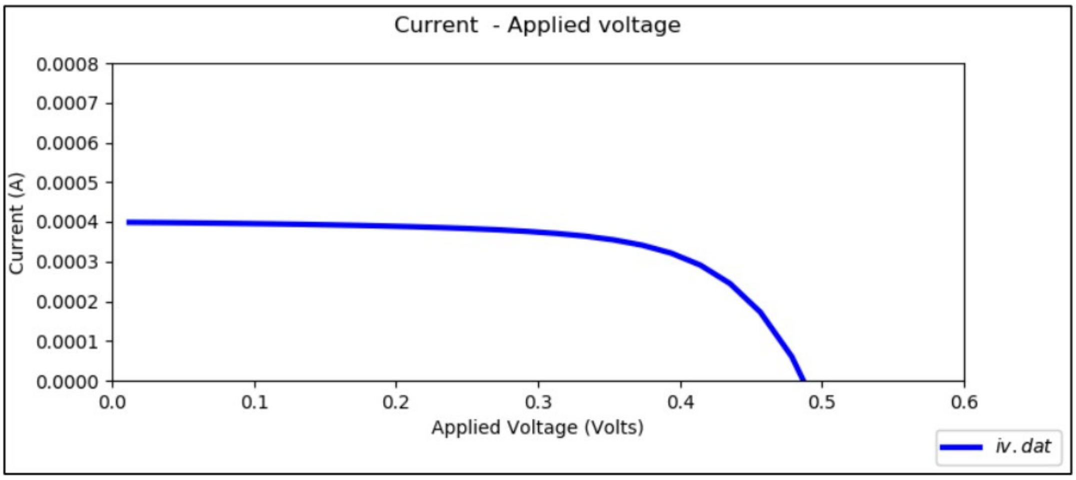

Figure 40 I-V Curve for Spinach Dye

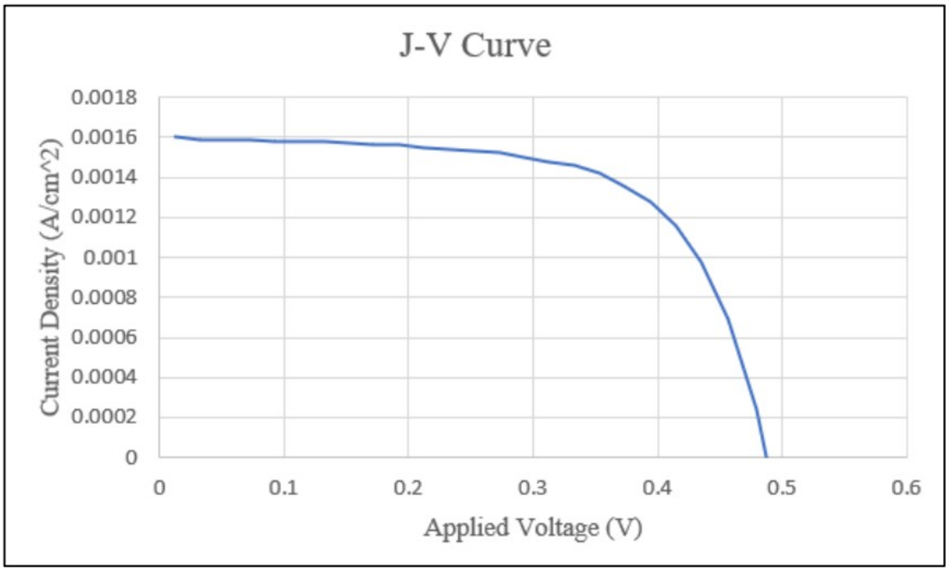

Figure 41 J-V Curve for Spinach Dye

Table 16 Simulation Result for Spinach Dye

Chlorophyll Dye	**Area DSSC (cm^2)**	**I_{sc} (mA)**	**J_{sc} (mA/cm^2)**	**V_{oc} (V)**
Spinach	0.25	0.4	1.6	0.479

4.1.7 Ti Plant Leaves

Figure 42 and 43 show I-V curve and J-V curve of simulation using Ti plant leaves as dye respectively. The value for Isc, Jsc and Voc is tabulated in Table 17.

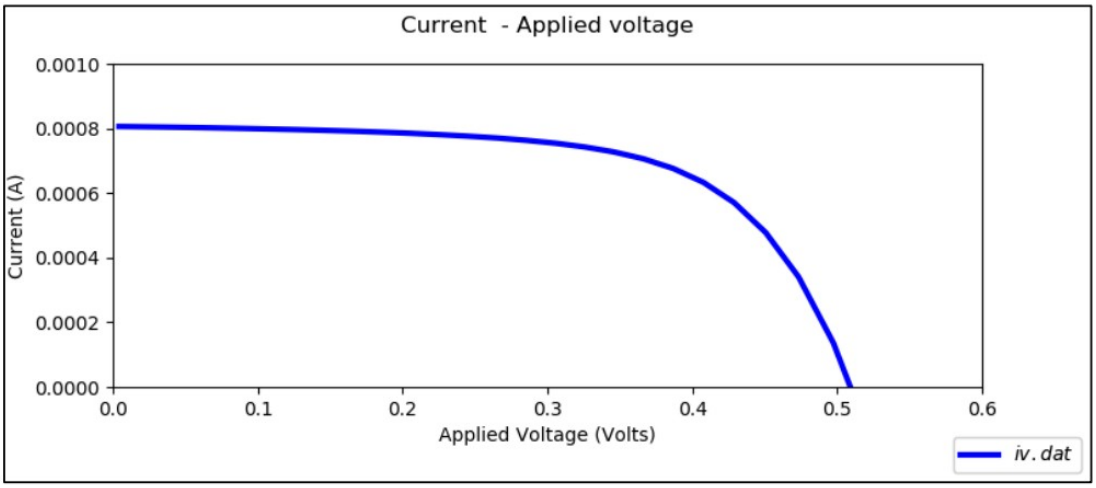

Figure 42 I-V Curve for Ti Plant Leaves Dye

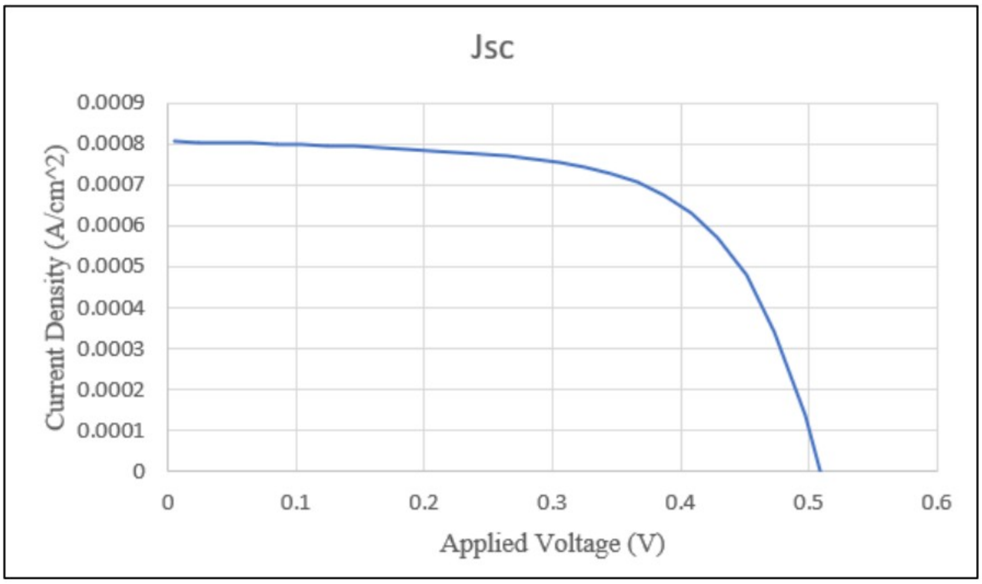

Figure 43 J-V Curve for Ti Plant Leaves Dye

Table 17 Simulation Result for Ti Plant Leaves Dye

Chlorophyll Dye	**Area DSSC (cm^2)**	**I_{sc} (mA)**	**J_{sc} (mA/cm^2)**	**V_{oc} (V)**
Ti Plant Leaves	1	0.8	0.8	0.523

4.1.8 Morning Glory Leaves

Figure 44 and 45 show I-V curve and J-V curve of simulation using Morning Glory leaves as dye respectively. The value for Isc, Jsc and Voc is tabulated in Table 18.

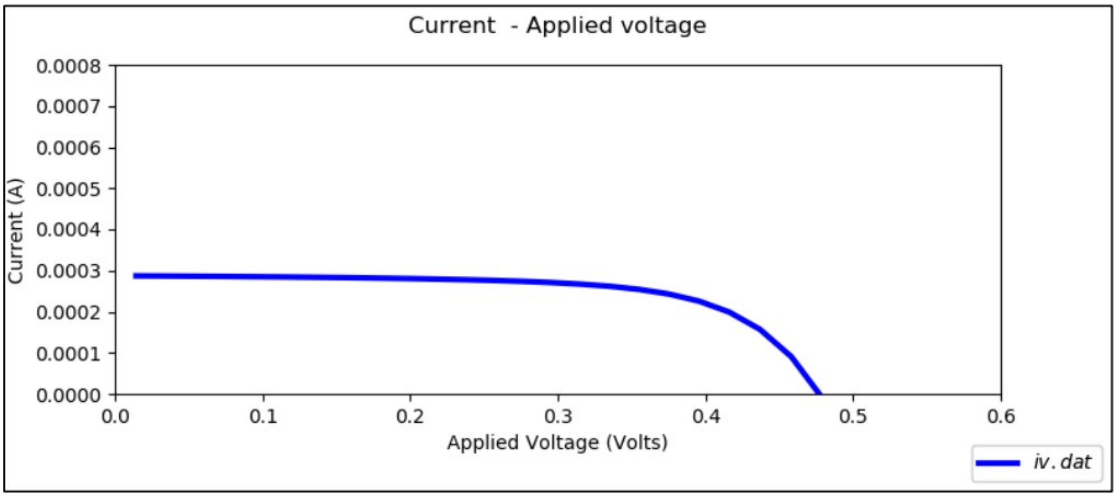

Figure 44 I-V Curve for Morning Glory Leaves Dye

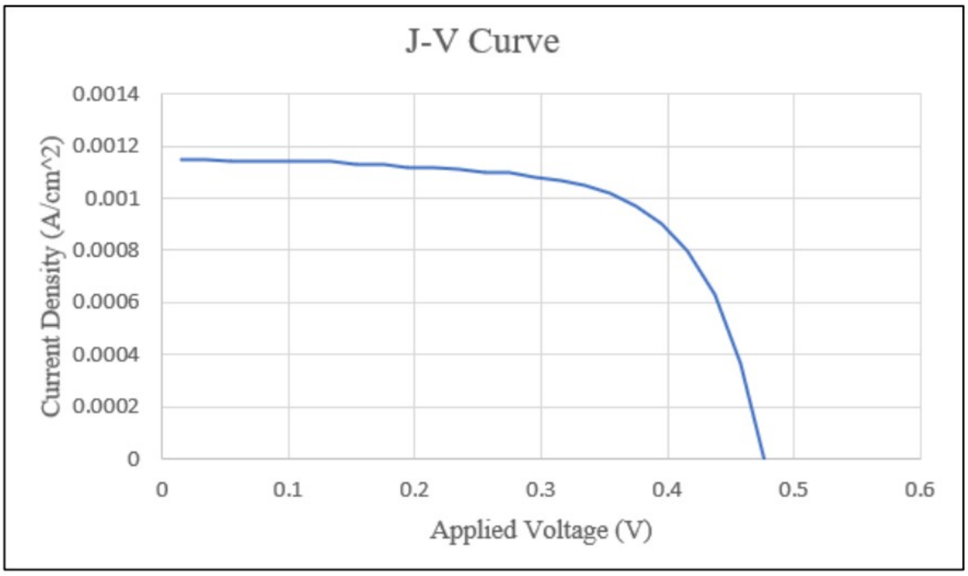

Figure 45 J-V Curve for Morning Glory Leaves Dye

Table 18 Simulation Result for Morning Glory Leaves Dye

Chlorophyll Dye	Area DSSC (cm^2)	I_{sc} (mA)	J_{sc} (mA/cm^2)	V_{oc} (V)
Morning Glory Leaves	0.25	0.287	1.148	0.48

4.1.9 Jatropha Curcas Leaves

Figure 46 and 47 show I-V curve and J-V curve of simulation using Jatropha Curcas leaves as dye respectively. The value for Isc, Jsc and Voc is tabulated in Table 19.

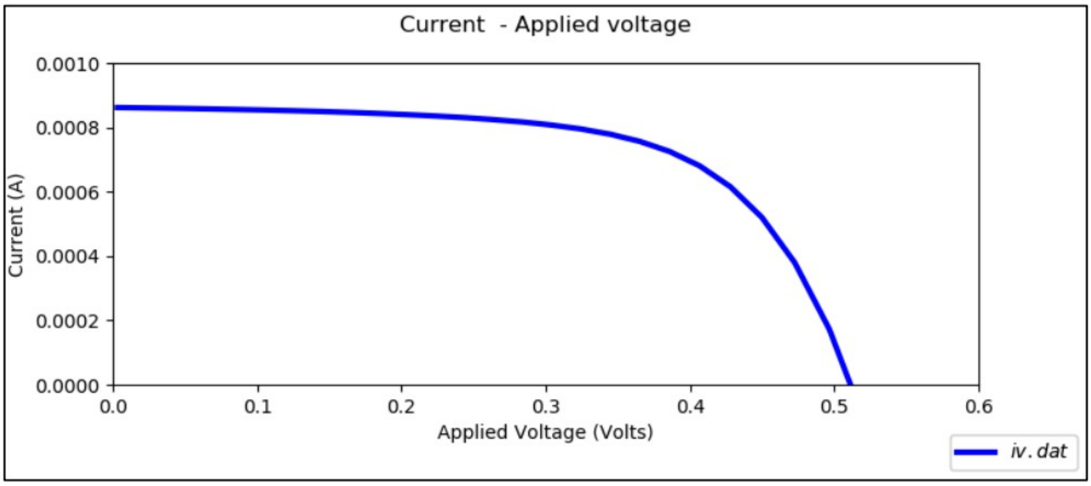

Figure 46 I-V Curve for Jatropha Curcas Leaves Dye

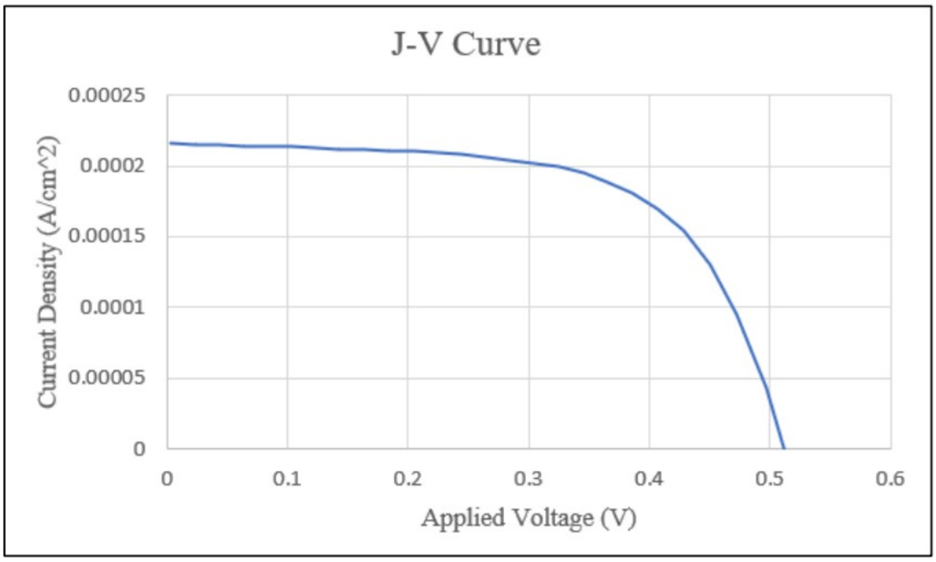

Figure 47 J-V Curve for Jatropha Curcas Leaves Dye

Table 19 Simulation Result for Jatropha Curcas Leaves Dye

Chlorophyll Dye	Area DSSC (cm^2)	I_{sc} (mA)	J_{sc} (mA/cm^2)	V_{oc} (V)
Jatropha Leaves	4	0.862	0.2155	0.523

4.1.10 Chinar Leaves

Figure 48 and 49 show I-V curve and J-V curve of simulation using Chinar leaves as dye respectively. The value for Isc, Jsc and Voc is tabulated in Table 20.

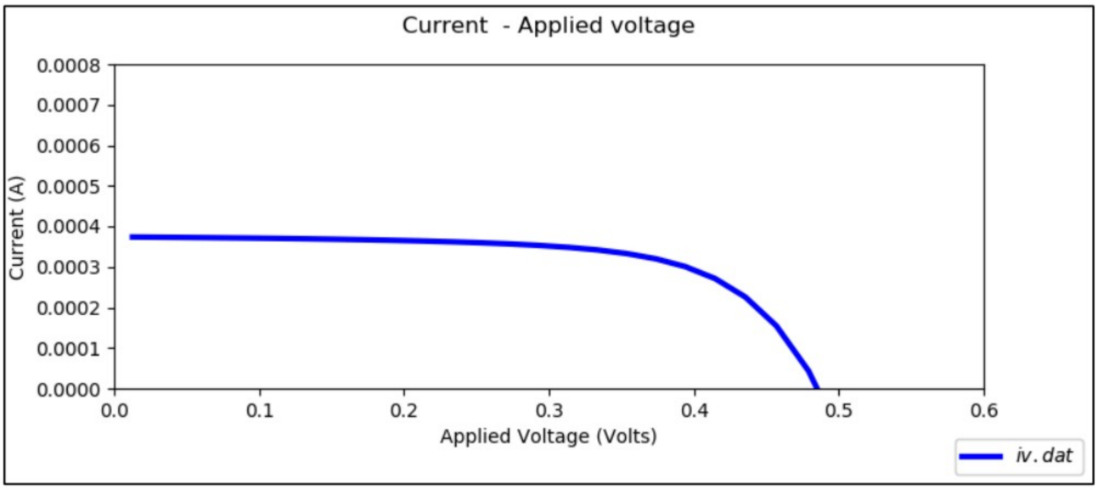

Figure 48 I-V Curve for Chinar Leaves Dye

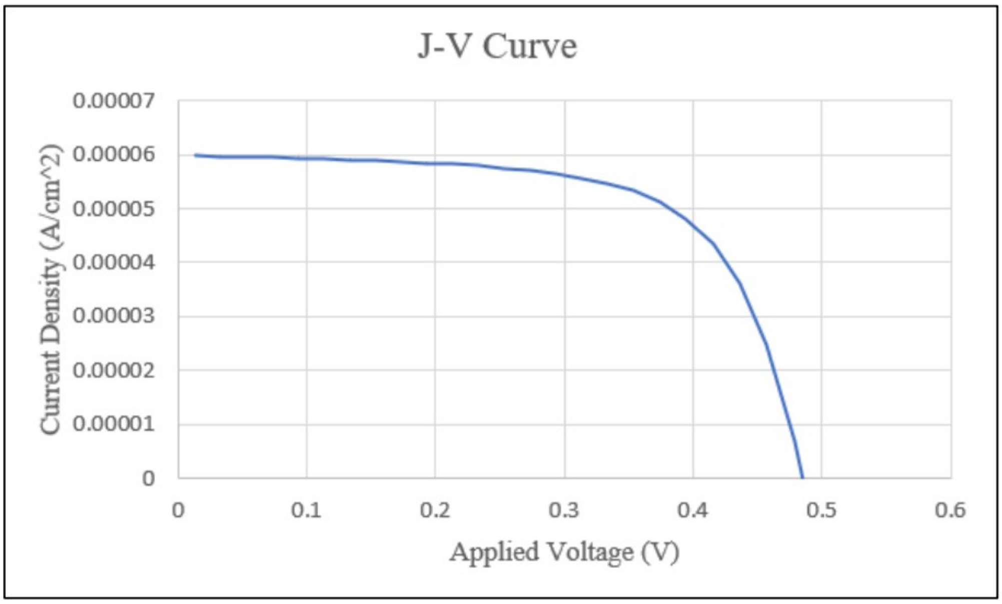

Figure 49 J-V Curve for Chinar Leaves Dye

Table 20 Simulation Result for Chinar Leaves Dye

Chlorophyll Dye	Area DSSC (cm^2)	I_{sc} (mA)	J_{sc} (mA/cm^2)	V_{oc} (V)
Chinar Leaves	6.25	0.374	0.05984	0.479

4.2 Discussion

The simulation result is been compared with the result of the previous research in Table 21 and Table 22. From all 10 samples chlorophyll dye, spinach dye shows the highest simulated value for J_{sc} which is 1.6 mA/cm^2 compared the others. While for simulated value for V_{oc}, Apricot leaves dye and Scent leaves dye show the highest compared to the others with 0.524 V.

Table 21 Comparison Between Research and Simulated Result for J_{sc}

Chlorophyll Dye	**Area DSSC (cm^2)**	**Research J_{sc} (mA/cm^2)**	**Simulated J_{sc} (mA/cm^2)**	**Difference J_{sc} (mA/cm^2)**	**Reference**
Neem Leaves	2.25	0.23	0.2667	0.0367	[10]
Apricot Leaves	2.56	0.771	0.271	-0.5	[11]
Papaya Leaves	4	0.06	0.2175	0.1575	[12]
Pawpaw Leaves	0.54	0.649	1.0648	0.4158	[13]
Scent Leaves	Assumed 1	0.044	0.71	0.666	[14]
Spinach	0.25	1.11	1.6	0.49	[15]
Ti Plant Leaves	1	1.3	0.8	-0.5	[16]
Morning Glory Leaves	0.25	0.85	1.148	0.298	[17]
Jatropha Carcus Leaves	4	0.042	0.2155	0.1735	[12]
Chinar Leaves	6.25	0.012	0.05984	0.04784	[18]

Table 22 Comparison Between Research and Simulated Result for V_{oc}

Chlorophyll Dye	**Area DSSC (cm^2)**	**Research V_{oc} (V)**	**Simulated V_{oc} (V)**	**Difference V_{oc} (V)**	**Reference**
Neem Leaves	2.25	0.467	0.5	0.033	[10]
Apricot Leaves	2.56	0.62	0.524	-0.096	[11]
Papaya Leaves	4	0.394	0.523	0.129	[12]
Pawpaw Leaves	0.54	0.504	0.5	-0.004	[13]
Scent Leaves	Assumed 1	0.466	0.524	0.058	[14]
Spinach	0.25	0.583	0.479	-0.104	[15]
Ti Plant Leaves	1	0.616	0.523	-0.093	[16]
Morning Glory Leaves	0.25	0.495	0.48	-0.015	[17]
Jatropha Carcus Leaves	4	0.35	0.523	0.173	[12]
Chinar Leaves	6.25	0.468	0.479	0.011	[18]

From Table 21 and Table 22 above, there are slightly difference between research result and simulated result. The highest difference for J_{sc} is scent leaves dye with 66.6%.

This might be because of the active area of DSSC where it is assumed for 1 cm^2. Another simulation has been conducted where all the size of active area of DSSC is assumed same which is 2.25 cm^2 and the result is tabulated in the Table 23.

Table 23 Simulated Result with Same Active Area

Chlorophyll Dye	**Area DSSC (cm^2)**	**Simulated I_{sc} (mA)**	**Simulated J_{sc} (mA/cm^2)**	**Simulated V_{oc} (V)**	**Reference**
Neem Leaves	2.25	0.6	0.2667	0.5	[10]
Apricot Leaves	2.25	0.695	0.3089	0.524	[11]
Papaya Leaves	2.25	0.87	0.3867	0.523	[12]
Pawpaw Leaves	2.25	0.575	0.2556	0.5	[13]
Scent Leaves	2.25	0.71	0.3156	0.524	[14]
Spinach	2.25	0.4	0.1778	0.479	[15]
Ti Plant Leaves	2.25	0.8	0.3556	0.523	[16]
Morning Glory Leaves	2.25	0.287	0.1276	0.48	[17]
Jatropha Carcus Leaves	2.25	0.862	0.3831	0.523	[12]
Chinar Leaves	2.25	0.374	0.1662	0.479	[18]

From above, Papaya leaves dye shows the highest value of J_{sc} with 0.3867 mA/cm^2 compared to the other chlorophyll dyes.

CHAPTER 5

CONCLUSION

5.1 Conclusion

In summary, this study conducts research on DSSC by finding the highest current-density (J-V) that can be produce from 10 samples chlorophyll dye by using General-purpose Photovoltaic Device Model (GPVDM) software. This software does not have sample structure of DSSC inside it, where we can use this software to identify the effectiveness of the software to simulate the dye-sensitized type solar cell.

From my observation, the highest simulated current-density (J-V) from 10 chlorophyll dyes that have been simulate for same active area is spinach with 1.6 mA/cm^2. Its value is the highest among other materials. The value of simulated short-circuit current-density (J_{sc}) are slightly difference to the value of experimented result J_{sc} from the published paper. It can be highly suggested that this GPVDM software is feasible to be used to simulate the DSSC structure.

As conclusion, this GPVDM can be considered as suitable for modelling the DSSC. However, mastering well in utilizing this software requires lots of effort and time since there are very limited sources available.

5.2 Recommendation

Based on our observation also, it can be suggested that one of the main important parameters in producing highest current density of DSSC is absorbance data. Therefore, lots of literature studies need to be massively done in order to improve the produced DSSC model in the future since not all the journal and research papers are mentioning all necessary constants.

REFERENCES

[1] B. G. Akinoglu, B. Tuncel, and V. Badescu, "Beyond 3rd generation solar cells and the full spectrum project. Recent advances and new emerging solar cells," *Sustain. Energy Technol. Assessments*, vol. 46, no. June 2020, p. 101287, 2021, doi: 10.1016/j.seta.2021.101287.

[2] P. Sudheer and C. Chengaiah, "Modelling and Simulation of Hybrid Transformer Less Grid-tied Inverters for Dye Sensitized Photovoltaic System," 2016, doi: 10.1016/j.procs.2016.05.228.

[3] S. Rudra, S. Sarker, and D. M. Kim, "Review on simulation of current–voltage characteristics of dye-sensitized solar cells," *J. Ind. Eng. Chem.*, vol. 80, pp. 516–526, 2019, doi: 10.1016/j.jiec.2019.08.030.

[4] S. Rudra, H. W. Seo, S. Sarker, and D. M. Kim, "Simulation and electrochemical impedance spectroscopy of dye-sensitized solar cells," *J. Ind. Eng. Chem.*, vol. 97, pp. 574–583, 2021, doi: 10.1016/j.jiec.2021.03.010.

[5] M. Mehrabian and S. Dalir, "Numerical simulation of highly efficient dye sensitized solar cell by replacing the liquid electrolyte with a semiconductor solid layer," *Optik (Stuttg).*, vol. 169, no. May, pp. 214–223, 2018, doi: 10.1016/j.ijleo.2018.05.059.

[6] M. Burgelman, P. Nollet, and S. Degrave, "Modelling polycrystalline semiconductor solar cells," *Thin Solid Films*, vol. 361, pp. 527–532, 2000, doi: 10.1016/S0040-6090(99)00825-1.

[7] M. T. Neukom *et al.*, "Consistent Device Simulation Model Describing Perovskite Solar Cells in Steady-State, Transient, and Frequency Domain," *ACS Appl. Mater. Interfaces*, vol. 11, no. 26, pp. 23320–23328, 2019, doi: 10.1021/acsami.9b04991.

[8] W. Farooq, A. D. Khan, A. D. Khan, and M. Noman, "Enhancing the power conversion efficiency of organic solar cells," *Optik (Stuttg).*, vol. 208, no. December 2019, p. 164093, 2020, doi: 10.1016/j.ijleo.2019.164093.

[9] S. Michael and A. Bates, "The design and optimization of advanced multijunction solar cells using the Silvaco ATLAS software package," *Sol. Energy Mater. Sol. Cells*, vol. 87, no. 1–4, pp. 785–794, 2005, doi: 10.1016/j.solmat.2004.07.051.

[10] N. T. Mary Rosana, D. JoshuaAmarnath, S. Anandan, and G. Saritha, "Environmental friendly photosensitizing materials for harvesting solar energy," *J. Mater. Environ. Sci.*, vol. 6, no. 8, pp. 2053–2059, 2015.

[11] S. A. Taya, T. M. El-Agez, K. S. Elrefi, and M. S. Abdel-Latif, "Dye-sensitized solar cells based on dyes extracted from dried plant leaves," *Turkish J. Phys.*, vol. 39, no. 1,

pp. 24–30, 2015, doi: 10.3906/fiz-1312-12.

[12] S. H. Pramono, E. Maulana, A. F. Prayogo, and R. Djatmika, "Characterization of dye-sensitized solar cell (DSSC) based on chlorophyll dye," *Int. J. Appl. Eng. Res.*, vol. 10, no. 1, pp. 193–205, 2015.

[13] M. Isah Kimpa, M. Momoh, K. Uthman Isah, H. Nawawi Yahya, and M. Muhammed Ndamitso, "Photoelectric Characterization of Dye Sensitized Solar Cells Using Natural Dye from Pawpaw Leaf and Flame Tree Flower as Sensitizers," *Mater. Sci. Appl.*, vol. 03, no. 05, pp. 281–286, 2012, doi: 10.4236/msa.2012.35041.

[14] D. Eli, "Chlorophyll and Betalain as Light-Harvesting Pigments for Nanostructured TiO₂ Based Dye-Sensitized Solar Cells," *J. Energy Nat. Resour.*, vol. 5, no. 5, p. 53, 2016, doi: 10.11648/j.jenr.20160505.11.

[15] S. A. Taya, "Dye-Sensitized Solar Cells Using Fresh and Dried Natural Dyes," *Int. J. Mater. Sci. Appl.*, vol. 2, no. 2, p. 37, 2013, doi: 10.11648/j.ijmsa.20130202.11.

[16] M. A. M. Al-Alwani, N. A. Ludin, A. B. Mohamad, A. A. H. Kadhum, M. M. Baabbad, and K. Sopian, "Optimization of dye extraction from Cordyline fruticosa via response surface methodology to produce a natural sensitizer for dye-sensitized solar cells," *Results Phys.*, vol. 6, pp. 520–529, 2016, doi: 10.1016/j.rinp.2016.08.013.

[17] H. Chang, H. M. Wu, T. L. Chen, K. D. Huang, C. S. Jwo, and Y. J. Lo, "Dye-sensitized solar cell using natural dyes extracted from spinach and ipomoea," *J. Alloys Compd.*, vol. 495, no. 2, pp. 606–610, 2010, doi: 10.1016/j.jallcom.2009.10.057.

[18] B. Q. Liu, X. P. Zhao, and W. Luo, "The synergistic effect of two photosynthetic pigments in dye-sensitized mesoporous TiO2 solar cells," *Dye. Pigment.*, vol. 76, no. 2, pp. 327–331, 2008, doi: 10.1016/j.dyepig.2006.09.004.

APPENDIX A
GANTT CHART FYP 1

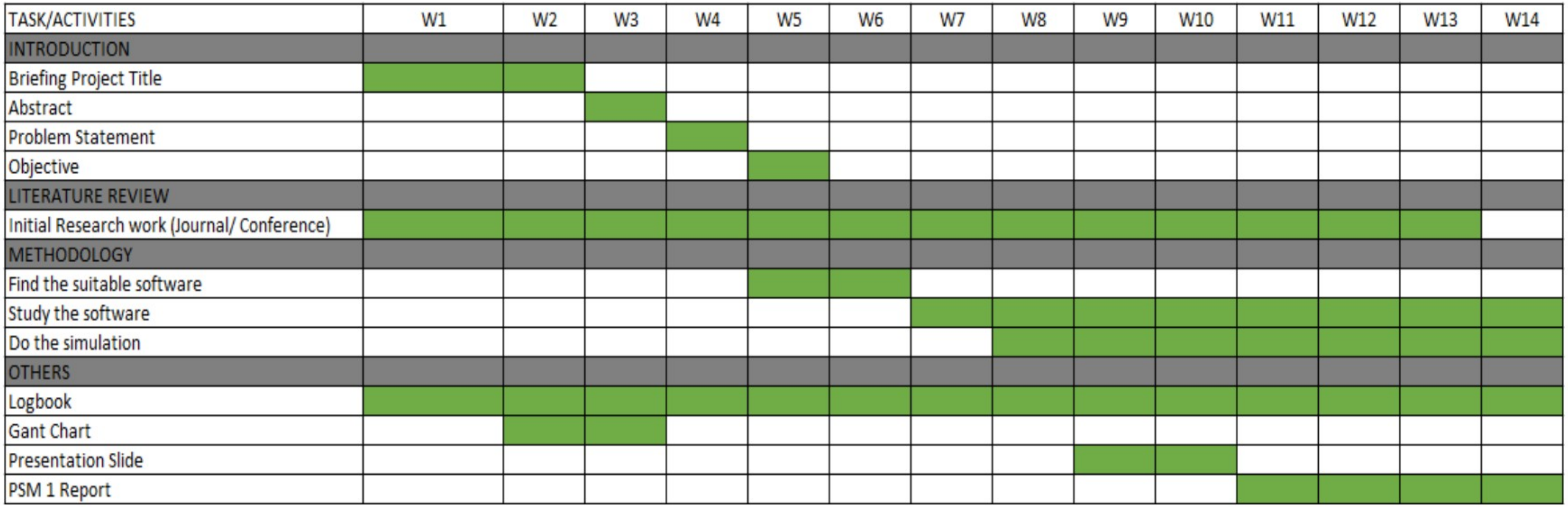

APPENDIX B
GANTT CHART FYP 2

TASK/ACTIVITIES	W1	W2	W3	W4	W5	W6	W7	W8	W9	W10	W11	W12	W13	W14
METHODOLOGY														
Find chlorophyll data	■	■	■	■	■	■								
Do the simulation						■	■	■	■	■	■	■	■	
Do analysis								■	■	■	■	■	■	
OTHERS														
Logbook	■	■	■	■	■	■	■	■	■	■	■	■	■	■
Gant Chart		■	■											
Presentation Slide													■	
PSM 2 Report (Thesis)											■	■	■	■